Table VIII. Positional Parameters and Their Estimated Standard Deviations for (C₅Me₅)Rh(PMe₂CH₂CH₂CH₂)Br

atom	x	y	z	B, Å^2
Rh	0.27554 (8)	0.2034 (1)	−0.00009 (6)	3.02 (2)
Br	0.2539 (1)	−0.0436 (2)	0.0820 (1)	6.53 (4)
P	0.2442 (3)	0.3424 (4)	0.1172 (2)	3.97 (8)
C15	0.427 (1)	0.221 (2)	0.0649 (9)	5.6 (4)
C13	0.358 (1)	0.337 (2)	0.193 (1)	7.2 (5)
C14	0.435 (1)	0.246 (2)	0.160 (1)	9.3 (6)
C11	0.217 (1)	0.545 (2)	0.102 (1)	7.3 (5)
C12	0.140 (1)	0.280 (2)	0.1779 (9)	6.7 (4)
C1	0.270 (1)	0.092 (2)	−0.1311 (8)	4.2 (3)
C2	0.3302 (9)	0.222 (2)	−0.1320 (7)	4.0 (3)
C3	0.268 (1)	0.351 (1)	−0.1146 (8)	4.2 (3)
C4	0.164 (1)	0.301 (2)	−0.1097 (7)	4.4 (3)
C5	0.1669 (9)	0.139 (1)	−0.1190 (8)	3.6 (3)
C6	0.302 (1)	−0.071 (2)	−0.146 (1)	7.0 (4)
C7	0.441 (1)	0.221 (2)	−0.1522 (9)	7.5 (5)
C8	0.301 (1)	0.514 (2)	−0.118 (1)	8.1 (5)
C9	0.071 (1)	0.397 (2)	−0.104 (1)	8.5 (5)
C10	0.079 (1)	0.036 (2)	−0.1187 (9)	7.3 (5)

Patterson map. The Molecular Structure Corporation SDP package was used for solution and refinement of the structure. A series of least-squares and difference Fourier maps revealed all 22 non-hydrogen atoms. Hydrogen atoms were placed with use of a difference Fourier map for methyl hydrogens or in idealized geometries for phenyl hydrogens. Final anisotropic refinement of all non-hydrogen atoms was carried out with fixed positional and thermal (B = 6.0) parameters for the 27 hydrogen atoms. Table III contains relevant bond distances and angles and Table VII positional parameters.

X-ray Structural Determination of (C₅Me₅)Rh(PMe₂CH₂CH₂CH₂)Br. Well-formed crystals of the cyclometallated phosphine derivative were prepared by slow evaporation of a hexane solution. The lattice constants were obtained from 25 centered reflections with values of χ between 10 and 45°. Cell reduction with the program TRACER revealed a monoclinic crystal system. The space group was assigned as $P2_1/n$ on the basis of systematic absences. Data were collected on the crystal in accord with the parameters in Table VI. The correctness of the choice of space group was confirmed by successful solution of the Patterson map. The Molecular Structure Corporation SDP package was used for solution and refinement of the structure. A series of least-squares and difference Fourier maps revealed all 18 non-hydrogen atoms. Hydrogen atoms were placed with use of a difference Fourier map for methyl hydrogens or in idealized geometries for phenyl hydrogens. Final anisotropic refinement of all non-hydrogen atoms was carried out with fixed positional and thermal (B = 6.0) parameters for the 27 hydrogen atoms. Table V contains relevant bond distances and angles and Table VIII lists positional parameters.

Supplementary Material Available: Tables of thermal parameters, positional parameters of placed atoms, bond distances and angles, structure factors, and least-squares planes (41 pages). Ordering information is given on any current masthead page.

Reactions of Re₂(CO)₈[μ-(L-L)] (L-L = dppm, dmpm) and Re₂(CO)₇[μ-(L-L)](NCMe) with Alkynes[1]

Kang-Wook Lee,[2a] William T. Pennington,[2b] A. Wallace Cordes,[2b] and Theodore L. Brown*[2a]

Contribution from the School of Chemical Sciences, University of Illinois, Urbana-Champaign, Urbana, Illinois 61801, and the Department of Chemistry, University of Arkansas, Fayetteville, Arkansas 72701. Received May 14, 1984

Abstract: The photochemical reaction of Re₂(CO)₈[μ-(L-L)] (L-L = dppm, dmpm) with terminal alkynes, RC≡CH (R = H, Ph), results in formation of (μ-H)Re₂(CO)₇[μ-(L-L)](η¹-C≡CRe₂) (I), (μ-H)Re₂(CO)₆[μ-(L-L)](μ-η¹,η²-C≡CR) (II), Re₂(CO)₅(L-L)(μ-η¹,η²-C(R)=CH₂)(μ-η¹,η²-C≡CR) (III), and Re₂(CO)₆[μ-(L-L)](μ-η¹,η²-C(R)=CH₂)(μ-η¹,η²-C≡CR) (IV). The yield for each product depends on the reaction time and the bridging ligand. I is the first isolated example of bridging hydrido, σ-bonded alkynyl di- or polynuclear compounds directly formed from alkyne. In the reaction of II with acetylenes, coordination of dppm has been rearranged to form a chelate in III. The kinetic studies for the photochemical reactions of Re₂(CO)₈[μ-(L-L)] and the isolated compounds I and II (L-L = dppm; R = Ph) with phenylacetylene indicate that the consecutive reactions occur with loss of one carbonyl ligand in each step: Re₂(CO)₈(μ-dppm) → I → II → III. The reaction of Re₂(CO)₈[μ-(L-L)] with Me₃NO in acetonitrile yields the acetonitrile-substituted complex Re₂(CO)₇[μ-(L-L)](NCMe) (VI) wherein the acetonitrile ligand is located trans to phosphorus. The thermal reaction of VI with phenylacetylene at low temperature (40 °C) yields I, in which the σ-bonded alkynyl ligand is cis to phosphorus. In the case of the reaction of Re₂(CO)₇(μ-dppm)(NCMe) with phenylacetylene, the isomer of I wherein σ-bonded alkynyl ligand is located trans to phosphorus is isolated as a minor product. I is transformed to II in a high-temperature thermal reaction (110 °C). The bridging alkynyl ligand of II undergoes a rapid fluxional process. The ΔG*꜀ value estimated from the coalescence temperature in the ¹³C NMR spectra is 10.5 kcal/mol. The structures of (μ-H)Re₂(CO)₇(μ-dmpm)(η¹-C≡CPh) (I_d) and Re₂(CO)₅(dppm)(μ-η¹,η²-CH=CH₂)(μ-η¹,η²-C≡CPh) (III꜀) were determined by conventional crystallographic techniques with Mo Kα X-rays. The crystals of I_d belong to the monoclinic space group P2₁/c with a = 12.594 (1) Å, b = 11.075 (1) Å, c = 18.461 (3) Å, β = 105.88 (1)°, V = 2476.8 (9) Å³, and z = 4. The crystals of III꜀ belong to the orthorhombic space group Pbca with a = 12.743 (2) Å, b = 15.974 (2) Å, c = 35.174 (4) Å, V = 7160 (2) Å³, and Z = 8.

As part of a broadly based study of the photochemical properties of dirhenium carbonyl compounds, we have shown that the

presence of a bridging phosphorus ligand such as bis(diphenylphosphino)methane (dppm), bis(dimethylphosphino)methane

Table I. Spectroscopic Data of $(\mu\text{-H})Re_2(CO)_7[\mu\text{-(L-L)}](\eta^1\text{-C}\equiv CR)$ (I)

L-L	R	IR $\nu_{CO,C\equiv C}$,[a] cm^{-1}	^{1}H NMR, δ	^{13}C{^{1}H},[d] δ	MS, m/e
dppm	H (I$_a$)	2106 (m), 2032 (s), 2017 (m, sh), 2007 (s), 1968 (m, br), 1942 (m, br), 1909 (m, br)	7.01–7.76 (m, 20 H),[b] 4.76 (q, 1 H, J = 12.7 Hz), 4.32 (q, 1 H, J = 11.3 Hz), 2.22 (d, 1 H, J = 3.1 Hz), –14.59 (dd, 1 H, J_{PH} = 17.2, 9.2 Hz)	196.2 (s, 1 c),[c,f] 191.2 (s, 1 C), 190.1 (d, 1 C, J_{PC} = 60.0 Hz), 184.4 (d, 1 C, J_{PC} = 12.0 Hz), 183.6 (s, 1 C), 182.9 (d, 1 C, J_{PC} = 58.0 Hz), 182.2 (d, 1 C, J_{PC} = 5.7 Hz)	980
	Ph (I$_b$)	2106 (m), 2096 (w, sh), 2027 (s), 2015 (s), 2007 (s), 1970 (m, br), 1944 (m, br), 1912 (s)	7.82–7.87 (m, 2 H),[b] 6.97–7.59 (m, 23 H), 4.65 (q, 1 H, J = 12.6 Hz), 4.29 (q, 1 H, J = 12.3 Hz), –14.42 (dd, 1 H, J_{PH} = 17.3, 9.1 Hz)	191.6 (d, 1 C, J_{PC} = 4.6 Hz),[b] 190.6 (d, 1 C, J_{PC} = 7.4 Hz), 189.6 (d, 1 C, J_{PC} = 60.9 Hz), 184.3 (d, 1 C, J_{PC} = 8.5 Hz), 183.8 (d, 1 C, J_{PC} = 4.5 Hz), 182.3 (d, 1 C, J_{PC} = 47.0 Hz), 182.1 (s, 1 C)	1056
dmpm	Ph (I$_d$)	2103 (m), 2093 (w, sh), 2025 (s), 2000 (s), 1975 (m), 1935 (m), 1907 (m)	7.05–7.23 (m, 5 H),[c] 3.13 (q, 1 H, J = 12.5 Hz), 2.79 (q, 1 H, J = 11.8 Hz), 1.91 (d, 3 H, J = 7.2 Hz), 1.89 (d, 3 H, J = 7.3 Hz), 1.86 (d, 3 H, J = 8.3 Hz), 1.77 (d, 3 H, J = 7.1 Hz), –15.85 (dd, 1 H, J = 14.4, 8.8 Hz)	191.1 (s, 2 C),[c,g] 191.0 (d, 1 C, J_{PC} = 58.8 Hz), 185.1 (d, 1 C, J_{PC} = 9.3 Hz), 183.7 (d, 1 C, J_{PC} = 9.3 Hz), 182.3 (s, 1 C), 183.2 (d, 1 C, J_{PC} = 44.3 Hz)	808

[a] Taken in toluene solution. [b] Taken in CDCl$_3$. [c] Taken in CD$_2$Cl$_2$. [d] Carbonyl region. [e] Molecular ion peak based on ^{187}Re. [f] Taken at –30 °C. [g] Taken at –80 °C.

(dmpm), bis(diphenylphosphino)ethane (dppe), and bis(dimethylphosphino)ethane (dmpe) leads to dramatically different photochemical behavior for Re$_2$(CO)$_8$[μ-(L-L)] as compared with Re$_2$(CO)$_{10}$.[3,4] For example, the products of reactions of Re$_2$-(CO)$_8$(μ-dmpm) or Re$_2$(CO)$_8$(μ-dppm) with ROH (R = H, Me) are quite stable dinuclear compounds, whereas the corresponding reactions with Re$_2$(CO)$_{10}$ lead to tetranuclear compounds, [Re-(CO)$_3$OH]$_4$ or [Re(CO)$_3$OMe]$_4$.[4,5] Mays and co-workers found that some products of reactions of Re$_2$(CO)$_{10}$ with terminal alkynes are unstable,[6] whereas the products from Re$_2$(CO)$_8$(μ-dppm) and Re$_2$(CO)$_8$(μ-dmpm) are stable, as described below.

The photochemical reactions of the Re$_2$(CO)$_8$[μ-(L-L)] compounds also differ from those of Re$_2$(CO)$_{10}$ in being much slower. In our earlier studies of the photochemical reactions of these dinuclear compounds we postulated that reactions of Re$_2$(CO)$_{10}$ occur via metal–metal bond homolysis, followed by reaction of the labile Re(CO)$_5$ radical intermediates and then recombination of the radicals.[4] The presence of the bridging phosphorus ligand reduces the likelihood of such a reaction, because the radicals are held in close proximity and recombine very rapidly. The much slower reactions of the Re$_2$(CO)$_8$[μ-(L-L)] compounds could thus be accounted for in terms of the relatively lower probability of a reaction of the radical intermediates with reagents present in the solution.

Alternatively, the photochemical reactions of Re$_2$(CO)$_8$[μ-(L-L)] compounds may occur via dissociative loss of CO. Recent studies of Mn$_2$(CO)$_{10}$ and other dinuclear metal carbonyl compounds show that CO dissociative loss does compete with metal–metal bond homolysis in flash photolyses, in which sunlamp radiation of wavelength >310 nm is employed.[7] Similar results are revealed in the work of other groups.[8] The dissociative loss

of CO may thus provide a favored pathway when metal–metal bond homolysis is disfavored. In this paper we explore the photochemical reactions of Re$_2$(CO)$_8$[μ-(L-L)] compounds with terminal alkynes and in addition the thermal reaction promoted by Me$_3$NO. The results, which include the preparation of several new and novel compounds, can be understood in terms of a dissociative loss of CO as the major initial pathway for reaction.

The formation of alkyne-substituted transition-metal complexes has been extensively studied.[9] Alkyne substitution for CO in dinuclear or cluster compounds can lead to several bonding modes; the principal possibilities involving two metal centers are sketched in Figure 1. Other bonding modes, involving more than two metal centers, are possible. Bonding modes E, F, or G can in principle be attained via oxidative addition of terminal (RC≡CH) or functionalized alkynes (e.g., Ph$_2$PC≡CR, R$_3$SnC≡CR).[10] However, few examples of a direct oxidative addition process are known;[11] η^1-bonded acetylides in dinuclear[12] or cluster compounds[13] are most commonly formed from activated metal–alkynyl compounds, e.g., Ag$^+$ $^-$C≡CR. Isolation of the first-stage product with bonding mode G is likely to be difficult in most instances because of strong driving forces for formation of E or F bonding

(1) (a) Work at the University of Illinois was sponsored by the National Science Foundation through Research Grants NSF CHE 81–19525 and 83–12331. (b) The work done at the University of Arkansas was partially supported by the National Science Foundation (EPSCOR ISP 8011447) and the State of Arkansas.

(2) (a) University of Illinois, Urbana-Champaign. (b) University of Arkansas.

(3) Lee, K.-W.; Pennington, W. T.; Cordes, A. W.; Brown, T. L. *Organometallics* **1984**, *3*, 404.

(4) Gard, D. R.; Brown, T. L. *J. Am. Chem. Soc.* **1982**, *104*, 6340.

(5) (a) Herberhold, M.; Süss, G. *Angew. Chem., Ind. Ed. Engl.* **1975**, *14*, 700. (b) Herberhold, M.; Süss, G.; Ellermann, J.; Gabelein, H. *Chem. Ber.* **1978**, *111*, 2931.

(6) Mays, M. J.; Prest, D. W.; Raithby, P. R. *J. Chem. Soc., Dalton Trans.* **1981**, 771.

(7) Herrick, R. S.; Brown, T. L. *Inorg. Chem.*, in press.

(8) (a) Hepp, A. F.; Wrighton, M. S. *J. Am. Chem. Soc.* **1983**, *105*, 5934. (b) Yesaka, H.; Kobayashi, T.; Yasufuku, K.; Nagakura, S. *J. Am. Chem. Soc.* **1983**, *105*, 6249. (c) Rothberg, L. J.; Cooper, N. J.; Peters, K. S.; Vaida, V. *J. Am. Chem. Soc.* **1982**, *104*, 3536. (d) Pöe, A.; Fox, A. *J. Am. Chem. Soc.* **1980**, *102*, 2497. (e) Hughey, J. L.; Anderson, C. P.; Meyer, T. J. *J. Organomet. Chem.* **1977**, *125*, C49. (f) Church, S. P.; Hermann, H.; Grevels, F.-W.; Schaffner, K. *J. Chem. Soc., Chem. Commun.* **1984**, 785.

(9) For recent reviews see: (a) Sappa, E.; Tiripicchio, A.; Braunstein, P. *Chem. Rev.* **1983**, *83*, 203. (b) Holton, J.; Lappert, M. F.; Pearce, R.; Yarrow, P. I. W. *Chem. Rev.* **1983**, *83*, 135. (c) Carty, A. J. *Pure Appl. Chem.* **1982**, *54*, 113.

(10) (a) Carty, A. J. *Adv. Chem. Ser.* **1982**, *196*, 163. (b) Smith, W. F.; Yule, J.; Taylor, N. J.; Paik, H. N.; Carty, A. J. *Inorg. Chem.* **1977**, *16*, 1593. (c) Cetinkaya, B.; Lappert, M. F.; McMeeking, J.; Palmer, D. E. *J. Chem. Soc., Dalton Trans.* **1973**, 1202.

(11) There are a few examples of mononuclear hydrido acetylides forming via alkyne substitution and C–H oxidative addition: (a) Brown, C. K.; Georgiou, D.; Wilkinson, G. *J. Chem. Soc. A* **1971**, 3120 and references therein. (b) Evans, W. J.; Engerer, S. C.; Coleson, K. M. *J. Am. Chem. Soc.* **1981**, *103*, 6672. (c) Collman, J. P.; Kang, J. W. *J. Am. Chem. Soc.* **1967**, *89*, 844. (d) Ittel, S. D.; Tolman, C. A.; English, A. D.; Jesson, J. P. *J. Am. Chem. Soc.* **1978**, *100*, 7577. (e) Nelson, J. N.; Jonassen, H. B.; Roundhill, D. M. *Inorg. Chem.* **1969**, *8*, 2591.

(12) (a) McEwan, D. M.; Pringle, P. G.; Shaw, B. L. *J. Chem. Soc., Chem. Commun.* **1982**, 859, 861, 1240, 581. (b) Puddephatt, R. J.; Thomson, M. A. *J. Organomet. Chem.* **1982**, *238*, 231. (c) Ciriano, M.; Howard, J. A. K.; Spencer, J. L.; Stone, F. G. A.; Wadepohl, H. *J. Chem. Soc., Dalton Trans.* **1979**, 1749.

(13) Bruce, M. I.; Abu Salah, O. M. *J. Chem. Soc., Chem. Commun.* **1972**, 858; **1974**, 688.

Reactions of $Re_2(CO)_8[\mu\text{-}(L\text{-}L)]$ with Alkynes

J. Am. Chem. Soc., Vol. 107, No. 3, 1985 633

Table II. Spectroscopic Data of $(\mu\text{-}H)Re_2(CO)_6[\mu\text{-}(L\text{-}L)](\mu\text{-}\eta^1,\eta^2\text{-}C\equiv CR)$ (II)

L-L	R	IR ν_{CO},^{a} cm^{-1}	^1H NMR, δ	$^{13}C\{^1H\}$ NMR,^{d} δ	MS, m/e^c
dppm	H (II$_a$)	2047 (s), 2017 (s), 1960 (s), 1936 (s, sh), 1928 (s)	7.09–7.35 (m, 20 H),^{b} 4.04 (s, 1 H), 2.92 (q, J = 11.4 Hz), 2.42 (q, J = 12.1 Hz), −12.20 (t, 1 H, J_{PH} = 10.0 Hz)	192.7 (s, 2 C),^{f} 188.9 (s, 2 C), 186.6 (t, 2 C, J_{PC} + $J_{P'C}$ = 71.2 Hz)	952
	Ph (II$_b$)	2046 (s), 2019 (s), 1960 (m), 1936 (s, sh), 1928 (s)	6.85–7.85 (m, 25 H),^{b} 3.11 (q, 1 H, J = 11.4 Hz), 2.57 (q, 1 H, J = 11.8 Hz), −11.85 (t, 1 H, J_{PH} = 10.0 Hz)	192.7 (s, 2 C),^{c} 189.8 (s, 2 C), 187.4 (t, 2 C, J_{PC} + $J_{P'C}$ = 71.3 Hz)	1028
dmpm	H (II$_c$)	2045 (s), 2013 (s), 1955 (s), 1933 (s), 1922 (vs)	3.94 (s, 1 H),^{b} 1.85 (q, 1 H, J = 11.9 Hz), 1.64 (s, 12 H), 1.12 (q, 1 H, J = 11.8 Hz), −12.75 (t, 1 H, J_{PH} = 10.0 Hz)	g	704
	Ph (II$_d$)	2045 (s), 2015 (s), 1954 (s), 1933 (s), 1922 (vs)	7.53 (dd, 2 H, J = 8.0, 1.6 Hz),^{c} 7.31–7.41 (m, 3 H), 1.88 (q, 1 H, J = 11.2 Hz), 1.66 (t, 6 H, J = 3.8 Hz), 1.55 (t, 6 H, J = 3.6 Hz), 1.23 (q, 1 H, J = 11.2 Hz), −12.42 (t, 1 H, J_{PH} = 10.3 Hz)	193.0 (s, 2 C),^{f} 190.3 (s, 2 C), 187.8 (t, 2 C, J_{PC} + $J_{P'C}$ = 72.1 Hz)	780

^{a} Taken in toluene solution. ^{b} Taken in CDCl$_3$. ^{c} Taken in CD$_2$Cl$_2$. ^{d} Carbonyl region. ^{e} Molecular ion peak based on ^{187}Re. ^{f} Taken in toluene-d_8. ^{g} Not taken.

Table III. Spectroscopic Data of $Re_2(CO)_5(dppm)(\mu\text{-}\eta^1,\eta^2\text{-}C(R)\text{=}CH_2)(\mu\text{-}\eta^1,\eta^2\text{-}C\equiv CPh)$ (III)

R	IR ν_{CO},^{a} cm^{-1}	^1H NMR,^{b} δ	^{13}C NMR,^{b} δ	FDMS, m/e^c
Ph(III$_b$)	2022 (s), 1944 (sh), 1942 (s), 1931 (s), 1915 (m), 1887 (w)	6.89–7.60 (m, 30 H), 4.87–4.97 (m, 3 H), 2.44 (s, 1 H)	200.1 (dd, 1 C, J_{PC} = 33.7, 12.9 Hz), 198.8 (s, 1 C), 197.0 (s, 1 C), 195.2 (s, 1 C), 194.0 (s, 1 C)	1102
H(III$_c$)	2022 (s), 1959 (w, sh), 1937 (m, sh), 1928 (s), 1914 (m), 1892 (w)	9.08 (dd, 1 H, J_{HH} = 15.7 and 11.0 Hz), 6.85–7.90 (m, 25 H), 5.14 (dd, 1 H, J_{HH} = 11.0 Hz, J_{PH} = 5.4 Hz), 5.00 (m, 1 H), 4.80 (m, 1 H), 3.05 (d, 1 H, J_{HH} = 15.7 Hz)	201.6 (dd, 1 C, J_{PC} = 32.4 and 14.0 Hz), 199.1 (s, 1 C), 197.3 (s, 1 C), 194.9 (s, 1 C), 193.0 (s, 1 C)	1026

^{a} Taken in toluene solution. ^{b} Taken in CDCl$_3$. ^{c} Molecular ion peak based on ^{187}Re.

modes, as well as further reaction with additional ligand.[14] However, we have obtained such a product, and we report herewith the crystal structure of $(\mu\text{-}H)Re_2(CO)_7(\mu\text{-}dmpm)(\eta^1\text{-}C\equiv CPh)$. In addition, we have also obtained the crystal structure of a novel subsequent reaction product, $Re_2(CO)_5(dppm)(\mu\text{-}\eta^1,\eta^2\text{-}CH\text{=}CH_2)(\mu\text{-}\eta^1,\eta^2\text{-}C\equiv CPh)$.

Results

Photochemical Reaction of $Re_2(CO)_{10}$ with Alkynes. The photochemical reaction of $Re_2(CO)_{10}$ with terminal alkynes proceeds rapidly under mild conditions, whereas the corresponding reaction with the internal alkynes does not yield significant alkyne-substituted product. Sunlamp photolysis of 1.0×10^{-2} M $Re_2(CO)_{10}$ in toluene or hexane in the presence of acetylene or phenylacetylene at ambient temperature yields $(\mu\text{-}H)Re_2(CO)_8(\mu\text{-}C\equiv CR)$ (R = H, Ph)[15] as a major product. The minor product(s) cannot be characterized because of fast decomposition.

Photochemical Reactions of $Re_2(CO)_8(\mu\text{-}dppm)$ and -$(\mu\text{-}dmpm)$ with Alkynes. Photolysis of $Re_2(CO)_8[\mu\text{-}(L\text{-}L)]$ (L-L = dppm, dmpm) in toluene in the presence of acetylene or phenylacetylene at ambient temperature for 12 h results in formation of $(\mu\text{-}H)Re_2(CO)_7[\mu\text{-}(L\text{-}L)](\eta^1\text{-}C\equiv CR)$ (I), $(\mu\text{-}H)Re_2(CO)_6[\mu\text{-}(L\text{-}L)]$-$(\mu\text{-}\eta^1,\eta^2\text{-}C\equiv CR)$ (II), $Re_2(CO)_5(dppm)(\mu\text{-}\eta^1,\eta^2\text{-}C(R)\text{=}CH_2)$-$(\mu\text{-}\eta^1,\eta^2\text{-}C\equiv CR)$ (III) and $Re_2(CO)_6[\mu\text{-}(L\text{-}L)](\mu\text{-}\eta^1,\eta^2\text{-}C(R)\text{=}CH_2)(\mu\text{-}\eta^1,\eta^2\text{-}C\equiv CR)$ (IV). All compounds have been characterized by IR, ^1H NMR, ^{13}C NMR, elemental analyses, and mass spectra. The yield of each compound depends on the reaction time and bridging ligand. The total isolated product yield is ca. 85–90%. The yield of IV is negligible with dppm and III is not found with dmpm. Less than 10% of reactants end as unidentified product(s).

(14) Hanson, B. E.; Johnson, B. F. G.; Lewis, J.; Raithby, P. R. *J. Chem. Soc., Dalton Trans.* **1980**, 1852.

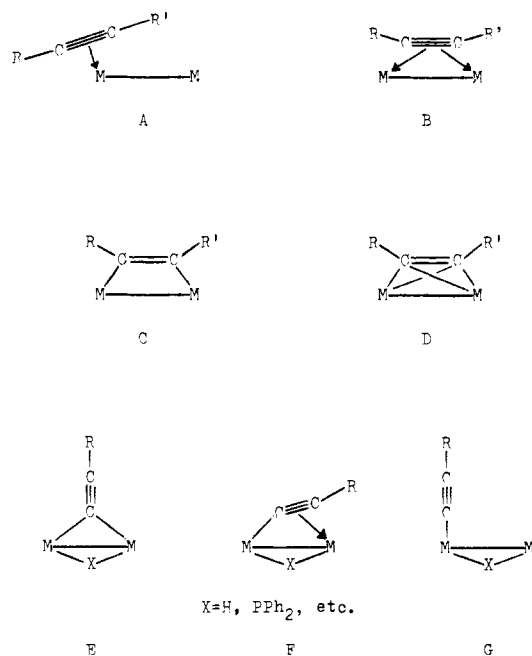(15) Nubel, P. O.; Brown, T. L. *Organometallics* **1984**, *3*, 29.

Figure 1. Principal modes of alkyne bonding to a binuclear metal system.

The spectroscopic data for I, II, and III are shown in Tables, I, II, and III, respectively.

The doublet of doublets for the bridging hydrido resonance of I in ^1H NMR suggests that the two phosphorus atoms are not symmetrically located with respect to the bridging hydride.[3] The ^{13}C NMR spectrum of I in the carbonyl region displays seven
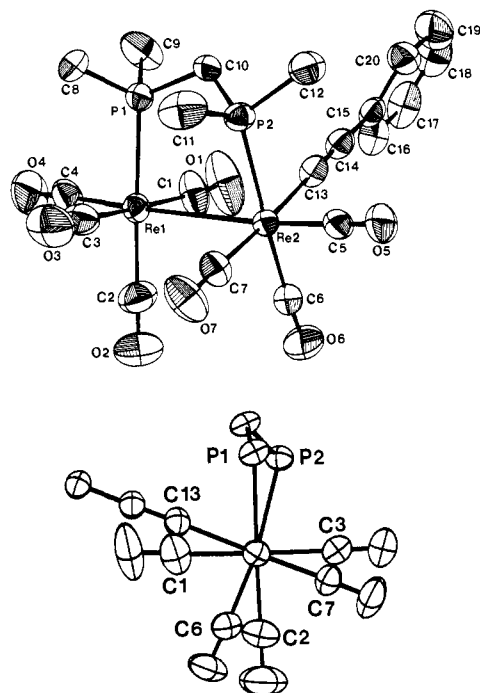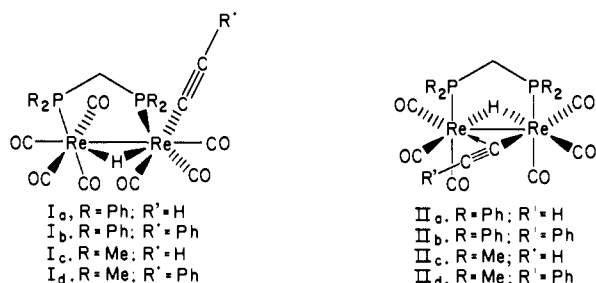
634 *J. Am. Chem. Soc., Vol. 107, No. 3, 1985*

Lee et al.

Figure 2. ORTEP drawings of $(\mu\text{-H})Re_2(CO)_7(\mu\text{-dmpm})(\eta^1\text{-C}\equiv CPh)$ (I_d) (top), and view down the Re(1)–Re(2) axis (bottom). The torsion angles are P(1)–Re(1)–Re(2)–P(2) = 15.1°, C(1)–Re(1)–Re(2)–C(13) = 21.9°, C(2)–Re(1)–Re(2)–C(6) = 25.7° and C(3)–Re(1)–Re(2)–C(7) = 22.3°.

peaks of equal intensity. The two doublets with a large coupling constant (44–60 Hz) correspond to the carbonyls trans to phosphorus atoms and the other five peaks with a small coupling constant (0–12 Hz) to the carbonyls cis to phosphorus atoms. However, it is difficult to determine the site (equatorial or axial) of the alkynyl group on the basis of these spectroscopic data. An X-ray crystal structure determination of the molecular structure of I_d was carried out. An ORTEP illustration is provided in Figure 2. The important bond lengths and angles are displayed in Table IV.

$I_a, R = Ph; R' = H$
$I_b, R = Ph; R' = Ph$
$I_c, R = Me; R' = H$
$I_d, R = Me; R' = Ph$

$II_a, R = Ph; R' = H$
$II_b, R = Ph; R' = Ph$
$II_c, R = Me; R' = H$
$II_d, R = Me; R' = Ph$

The ^{13}C NMR spectrum of II_a at –77 °C shows four singlets at δ 193.9, 191.7, 190.1, and 188.0 and two doublets of doublets at δ 187.7 (J_{PC} = 63.9 Hz) and 186.2 (J_{PC} = 75.6 Hz). The former four peaks correspond to the carbonyls cis to phosphorus atoms and the latter two peaks to those trans to phosphorus atoms. The triplet for the hydrido resonance in the ^1H NMR is consistent with a symmetrical disposition of the two phosphorus atoms with respect to the bridging hydride. The IR spectrum of II in the CO stretching region is very similar to that of $(\mu\text{-H})Re_2(CO)_6(\mu\text{-dppm})(\mu\text{-OH})$, the molecular structure of which has been determined in our laboratory.[3] On the basis of these spectroscopic data, we propose that II has a structure analogous to that of $(\mu\text{-H})Re_2(CO)_6(\mu\text{-dppm})(\mu\text{-OH})$, as shown above. Photolysis of I in toluene at ambient temperature or reflux of I in toluene for 3 h quantitatively yields II. The reverse reaction of II into I under 50 psig of CO pressure by photolysis or thermolysis (100 °C) is not observed.

The structure of III can be ascertained by comparison with that of $Re_2(CO)_5(dppm)(\mu\text{-}\eta^1,\eta^2\text{-CH}=CH_2)(\mu\text{-}\eta^1,\eta^2\text{-C}\equiv CPh)$ (III_c),

Table IV. Selected Bond Distances and Bond Angles for $(\mu\text{-H})Re_2(CO)_7(\mu\text{-dmpm})(\eta^1\text{-C}\equiv CPh)$ (I_d)

(a) Bond Distances (Å)

Re(1)–Re(2)	3.416 (1)	P(1)–C(10)	1.829 (6)
Re(1)–P(1)	2.440 (2)	P(2)–C(10)	1.824 (6)
Re(1)–C(1)	1.980 (8)	P(2)–C(11)	1.838 (8)
Re(1)–C(2)	1.944 (8)	P(2)–C(12)	1.809 (8)
Re(1)–C(3)	1.975 (8)	C(1)–O(1)	1.14 (1)
Re(1)–C(4)	1.944 (7)	C(2)–O(2)	1.143 (9)
Re(2)–P(2)	2.429 (1)	C(3)–O(3)	1.115 (9)
Re(2)–C(5)	1.913 (6)	C(4)–O(4)	1.126 (8)
Re(2)–C(6)	1.940 (7)	C(5)–O(5)	1.127 (7)
Re(2)–C(7)	1.929 (7)	C(6)–O(6)	1.133 (9)
Re(2)–C(13)	2.126 (7)	C(7)–O(7)	1.156 (8)
P(1)–C(8)	1.807 (8)	C(13)–C(14)	1.200 (9)
P(1)–C(9)	1.824 (8)	C(14)–C(15)	1.432 (9)

(b) Bond Angles (deg)

Re(2)–Re(1)–P(1)	87.58 (4)	C(2)–Re(1)–C(3)	89.0 (3)
Re(2)–Re(1)–C(1)	85.5 (2)	C(2)–Re(1)–C(4)	93.3 (3)
Re(2)–Re(1)–C(2)	88.1 (2)	C(3)–Re(1)–C(4)	91.1 (3)
Re(2)–Re(1)–C(3)	91.2 (2)	P(2)–Re(2)–C(5)	90.7 (2)
Re(2)–Re(1)–C(4)	177.4 (2)	P(2)–Re(2)–C(6)	170.2 (2)
Re(1)–Re(2)–P(2)	84.01 (4)	P(2)–Re(2)–C(7)	96.2 (2)
Re(1)–Re(2)–C(5)	174.6 (2)	P(2)–Re(2)–C(13)	82.0 (2)
Re(1)–Re(2)–C(6)	91.5 (2)	C(5)Re(2)–C(6)	93.9 (3)
Re(1)–Re(2)–C(7)	88.0 (2)	C(5)–Re(2)–C(7)	91.6 (3)
Re(1)–Re(2)–C(13)	88.2 (2)	C(5)–Re(2)–C(13)	92.1 (3)
Re(1)–P(1)–C(8)	115.0 (3)	C(6)–Re(2)–C(7)	92.4 (3)
Re(1)–P(1)–C(9)	114.3 (3)	C(6)–Re(2)–C(13)	89.2 (3)
Re(1)–P(1)–C(10)	115.8 (2)	C(7)–Re(2)–C(13)	175.9 (2)
Re(2)–P(2)–C(10)	113.6 (2)	Re(2)–C(13)–C(14)	178.7 (6)
Re(2)–P(2)–C(11)	116.7 (3)	C(13)–C(14)–C(15)	178.9 (6)
Re(2)–P(2)–C(12)	114.2 (2)	Re(1)–C(1)–O(1)	176 (1)
P(1)–C(10)–P(2)	117.7 (3)	Re(1)–C(2)–O(2)	179.3 (8)
P(1)–Re(1)–C(1)	88.7 (3)	Re(1)–C(3)–O(3)	177.1 (8)
P(1)–Re(1)C(2)	175.3 (2)	Re(1)–C(4)–O(4)	176.8 (8)
P(1)–Re(1)–C(3)	89.3 (2)	Re(2)–C(5)–O(5)	177.7 (6)
P(1)–Re(1)–C(4)	91.2 (2)	Re(2)–C(6)–O(6)	177.1 (6)
C(1)–Re(1)–C(2)	92.8 (4)	Re(2)–C(7)–O(7)	177.9 (7)
C(1)–Re(1)–C(3)	176.2 (3)		
C(1)–Re(1)–C(4)	92.2 (3)		

which is formed from the reaction of II_b with acetylene, as discussed later.

The ^{13}C NMR spectrum of IV_d at ambient temperature (δ 196.2 (d, J = 8.2 Hz), 195.7 (d, J = 6.9 Hz), 195.5 (d, J = 7.8 Hz), 192.9 (s), 189.1 (d, J = 72.5 Hz), 187.6 (d, J = 65.7 Hz)) indicates that four carbonyls are located cis to phosphorus atoms and two carbonyls trans to phosphorus atoms. The fast atom bombardment mass spectrum reveals the molecular ion of $Re_2(CO)_6(dmpm)$-$(PhC\equiv CH)_2$. ^1H NMR shows the presence of two protons. However, they are not metal hydride peaks and there is no splitting between them. On the basis of these spectroscopic data, two possible structures for IV appear most likely:

$IV_a, R = Ph; R' = H$
$IV_b, R = Ph; R' = Ph$
$IV_c, R = Me; R' = H$
$IV_d, R = Me; R' = Ph$
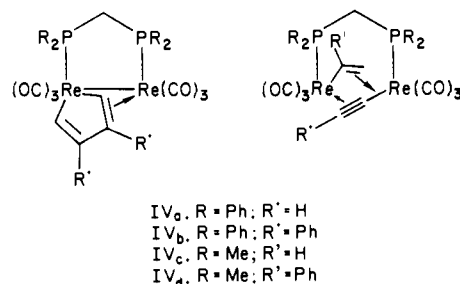
IV_c which may be formed from $Re_2(CO)_8(\mu\text{-dmpm})$ and acetylene could not be isolated because of decomposition on TLC plates. However, the ^1H NMR spectrum of the reaction mixture shows a vinylic proton pattern [δ 6.30 (dd, J = 17.0 and 10.9 Hz), 5.70 (d, J = 17.0 Hz), 5.45 (d, J = 10.9 Hz)]. If these peaks are due to IV_c, the bridging alkenyl–alkynyl structure is more likely. When II_d was irradiated in the presence of phenylacetylene in an IR cell, IV_d was the dominant product (~70%). The fact that the alkynyl
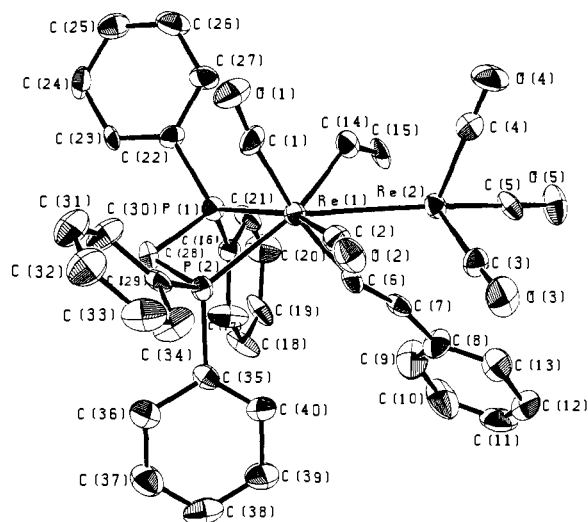
Figure 3. ORTEP drawing of $Re_2(CO)_5(dppm)(\mu-\eta^1,\eta^2-CH=CH_2)(\mu-\eta^1,\eta^2-C\equiv CPh)$ (III$_c$).

ligand cannot be removed by reductive elimination also suggests formation of a bridging alkenyl–alkynyl structure. Unfortunately, IV$_{a,b}$ cannot be separated on TLC. However, the field desorption mass spectrum (FDMS) of the reaction mixture shows the presence of an ion that could be the parent molecular ion of IV$_{a,b}$.

Photolysis of I$_d$ in toluene for 24 h quantitatively yields II$_d$; the same reaction of I$_d$ with phenylacetylene yields a mixture of II$_d$ and IV$_d$.

Reaction of II$_b$ with Acetylene and Triphenylphosphine. We have not been successful in obtaining a single crystal of III$_b$ suitable for X-ray structure determination. Since the photochemical reaction of II$_b$ with phenylacetylene yields III$_b$, the corresponding reaction with acetylene might be expected to yield a product similar to III$_b$.

Photolysis of II$_b$ with acetylene in toluene for 12 h leads to formation of a yellow crystalline substance, III$_c$. The ^{13}C NMR spectrum shows four singlets and a doublet of doublets ($J = 32.4$ and 14.0 Hz) of equal intensity, suggesting that only one carbonyl is located trans to phosphorus and that the two phosphorus atoms of dppm may be bonded to the same rhenium. The molecular structure was determined by X-ray methods; an ORTEP drawing is shown in Figure 3, and the important bond lengths and angles are displayed in Table V.

III$_a$. R = H; R' = H
III$_b$. R = Ph; R' = Ph
III$_c$. R = Ph; R' = H
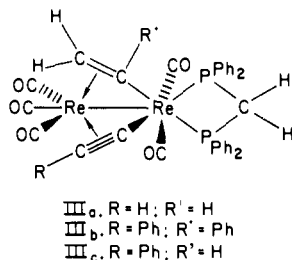
Reflux of II$_b$ with an excess of PPh$_3$ in toluene for 3 h results in formation of $(\mu-H)Re_2(CO)_5(\mu-dppm)(\mu-C\equiv CPh)(PPh_3)$ (V), characterized by IR, ^1H NMR, ^{13}C NMR, elemental analyses, and mass spectrum (refer to Experimental Section). The ^{13}C NMR indicates that only one carbonyl is located trans to phosphorus. The absence of a doublet of doublets indicates that rearrangement of the dppm bonding has not occurred. It is believed that PPh$_3$ substitutes for the carbonyl trans to phosphorus, giving the following structure
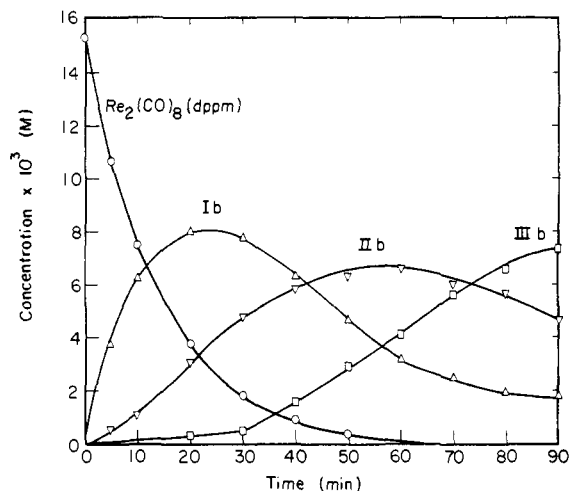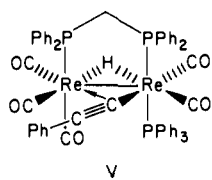

V

Figure 4. Concentration vs. time for the photochemical reaction of $Re_2(CO)_8(\mu-dppm)$ with phenylacetylene in a 0.2-mm IR cell with a sunlamp source.
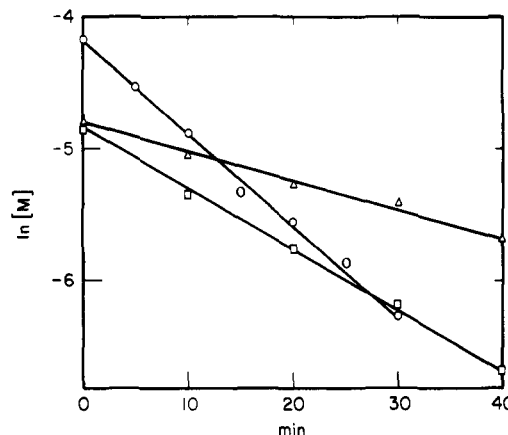

Figure 5. Relationship between ln [M] and time: (O) $Re_2(CO)_8(\mu-dppm)$; (□) I$_b$; (△) II$_b$.

The system is probably fluxional at room temperature, as observed for II$_b$. However, this point was not investigated, nor do we know whether there is a strong preference for location of the PPh$_3$ on the other rhenium from that shown in V.

Kinetic Studies of the Photochemical Reactions of Re$_2$(CO)$_8$-(μ-dppm), I$_b$, and II$_b$. In the hope that the course of the photochemical reaction between $Re_2(CO)_8(\mu-dppm)$ and alkynes might be more fully elucidated, the kinetics of the reactions of Re$_2$-(CO)$_8(\mu-dppm)$, I$_b$, and II$_b$ with phenylacetylene have been studied with IR spectroscopy. The extinction coefficients of $Re_2(CO)_8$-(μ-dppm), I$_b$, II$_b$, and III$_b$ at 2073, 2106, 2046, and 1887 cm^{-1}, respectively, have been determined with authentic samples. IR spectra were recorded at 5–10 min intervals during sunlamp photolysis of 1.53×10^{-2} M $Re_2(CO)_8(\mu-dppm)$ and 0.360 M phenylacetylene in toluene. A plot of the concentrations of $Re_2(CO)_8(\mu-dppm)$, I$_b$, II$_b$, and III$_b$ as a function of time is displayed in Figure 4. In separate experiments involving Re$_2$-(CO)$_8(\mu-dppm)$, I$_b$, and II$_b$ as initial reactants, it was established that the rates of disappearance of each reactant in the presence of an excess phenylacetylene show pseudo-first-order dependence, as shown in Figure 5, with first-order rate constants of 7.03×10^{-2}, 4.75×10^{-2}, and 2.40×10^{-2} min^{-1}, respectively. The rate of disappearance of $Re_2(CO)_8(\mu-dppm)$ is essentially independent of the concentration of phenylacetylene when the latter is present in greater than fivefold excess.

Preparation of Re$_2$(CO)$_7$[μ-(L-L)](NCMe) and Their Reactions with Phosphine Ligands. The reaction of $Re_2(CO)_8[\mu-(L-L)]$ with 1.2 equiv of anhydrous trimethylamine N-oxide in acetonitrile at ambient temperature gives the acetonitrile complex Re$_2$(CO)$_7$-[μ-(L-L)](NCMe), characterized by IR, ^1H NMR, ^{13}C NMR, and mass spectra, in nearly quantitative yield. While Re$_2$-

Table V. Selected Bond Distances and Bond Angles for
Re$_2$(CO)$_5$(dppm)(μ-η^1,η^2-CH=CH$_2$)(μ-η^1,η^2-C≡CPh) (III$_c$)

(a) Bond Distances (Å)

Re(1)-Re(2)	2.895 (1)	P(1)-C(16)	1.81 (2)
Re(1)-P(1)	2.441 (3)	P(1)-C(22)	1.81 (1)
Re(1)-P(2)	2.422 (4)	P(1)-C(28)	1.87 (2)
Re(1)-C(1)	1.92 (2)	P(2)-C(28)	1.82 (1)
Re(1)-C(2)	1.91 (2)	P(2)-C(29)	1.79 (1)
Re(1)-C(6)	2.09 (2)	P(2)-C(35)	1.80 (1)
Re(1)-C(14)	2.12 (2)	C(1)-O(1)	1.16 (2)
Re(2)-C(3)	1.92 (2)	C(2)-O(2)	1.22 (2)
Re(2)-C(4)	1.96 (2)	C(3)-O(3)	1.13 (2)
Re(2)-C(5)	1.89 (2)	C(4)-O(4)	1.10 (2)
Re(2)-C(6)	2.34 (1)	C(5)-O(5)	1.14 (2)
Re(2)-C(7)	2.48 (2)	C(6)-C(7)	1.24 (2)
Re(2)-C(14)	2.27 (1)	C(7)-C(8)	1.47 (2)
Re(2)-C(15)	2.38 (2)	C(14)-C(15)	1.36 (2)

(b) Bond Angles (deg)

Re(2)-Re(1)-P(1)	125.8 (1)	C(3)-Re(2)-C(4)	89.8 (7)
Re(2)-Re(1)-P(2)	145.02 (8)	C(3)-Re(2)-C(5)	92.9 (7)
Re(2)-Re(1)-C(1)	116.9 (5)	C(3)-Re(2)-C(6)	95.8 (6)
Re(2)-Re(1)-C(2)	72.9 (5)	C(3)-Re(2)-C(14)	147.5 (6)
Re(2)-Re(1)-C(6)	53.2 (4)	C(3)-Re(2)-C(15)	171.7 (6)
Re(2)-Re(1)-C(14)	51.1 (4)	C(4)-Re(2)-C(5)	87.9 (6)
Re(1)-Re(2)-C(3)	104.5 (5)	C(4)-Re(2)-C(6)	153.7 (6)
Re(1)-Re(2)-C(4)	108.2 (5)	C(4)-Re(2)-C(14)	87.6 (6)
Re(1)-Re(2)-C(5)	156.0 (4)	C(4)-Re(2)-C(15)	98.5 (6)
Re(1)-Re(2)-C(6)	45.5 (4)	C(5)-Re(2)-C(6)	117.3 (6)
Re(1)-Re(2)-C(7)	75.1 (4)	C(5)-Re(2)-C(14)	119.3 (6)
Re(1)-Re(2)C(14)	46.5 (4)	C(5)-Re(2)-C(15)	87.8 (6)
Re(1)-Re(2)-C(15)	72.6 (3)	C(6)-Re(2)-C(14)	74.0 (5)
P(1)-Re(1)-P(2)	68.9 (1)	C(6)-Re(2)-C(15)	76.6 (5)
P(1)-Re(1)-C(1)	91.2 (4)	C(14)-Re(2)-C(15)	33.7 (6)
P(1)-Re(1)-C(2)	158.9 (5)	Re(1)-P(1)-C(28)	95.0 (4)
P(1)-Re(1)-C(6)	93.5 (4)	Re(1)-P(2)-C(28)	97.0 (5)
P(1)-Re(1)-C(14)	87.7 (4)	P(1)-C(28)-P(2)	96.4 (4)
P(2)-Re(1)-C(1)	91.8 (5)	Re(1)-C(6)-C(7)	162 (1)
P(2)-Re(1)-C(2)	90.1 (5)	Re(1)-C(6)-Re(2)	81.2 (5)
P(2)-Re(1)-C(6)	98.4 (4)	C(6)-C(7)-C(8)	164 (2)
P(2)-Re(1)-C(14)	156.6 (4)	Re(1)-C(14)-C(15)	129 (1)
C(1)-Re(1)-C(2)	87.2 (6)	Re(1)-C(14)-Re(2)	82.4 (5)
C(1)-Re(1)-C(6)	169.8 (6)	Re(2)-C(6)-C(7)	81.5 (9)
C(1)-Re(1)-C(14)	88.5 (7)	Re(2)-C(14)-C(15)	78 (1)
C(2)-Re(1)-C(6)	91.7 (6)	Re(2)-C(15)-C(14)	68.6 (8)
C(2)-Re(1)-C(14)	113.2 (6)	Re(1)-C(1)-O(1)	174 (1)
C(6)-Re(1)-C(14)	82.6 (6)	Re(1)-C(2)-O(2)	166 (1)
		Re(2)-C(3)-O(3)	178 (2)
		Re(2)-C(4)-O(4)	176 (2)
		Re(2)-C(5)-O(5)	179 (1)

(CO)$_7$(μ-dmpm)(NCMe) (VI$_b$) is unstable in air, Re$_2$(CO)$_7$(μ-dppm)(NCMe) (VI$_a$) can be isolated as air-stable yellow crystal by preparative TLC. The ZAB-FAB (fast atom bombardment) mass spectrum shows molecular ions (m/e 995 based on ^{187}Re). The ^{1}H NMR spectrum of VI$_a$ in CDCl$_3$ shows a singlet at δ 2.38 and a triplet at δ 4.15. The former is assigned to the acetonitrile protons and the latter to the methylene protons of dppm. The ^{13}C NMR spectrum shows five doublets at δ 209.0 (2 C, J_{PC} = 6.4 Hz), 206.9 (2 C, J_{PC} = 8.6 Hz), 199.4 (1 C, J_{PC} = 48.9 Hz), 193.5 (1 C, J_{PC} = 7.0 Hz), and 192.6 (1 C, J_{PC} = 3.6 Hz). Only one peak with a large coupling constant (199.4 ppm, J_{PC} = 48.9 Hz) corresponds to the carbonyl trans to phosphorus. These spectroscopic data indicate that the acetonitrile ligand is located trans to phosphorus


VI$_a$
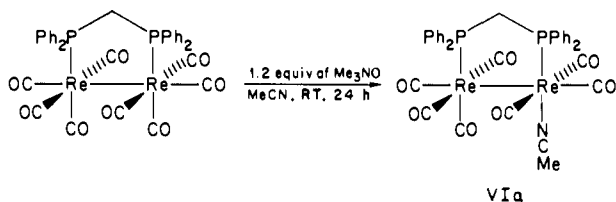
When an excess (3–5 equiv) of Me$_3$NO is employed in the reaction, the IR spectrum of the mixture does not reveal the presence

of a more highly substituted product such as Re$_2$(CO)$_6$(μ-dppm)(NCMe)$_2$.

The reaction of VI$_a$ with phosphine ligands such as PMe$_3$, PPh$_3$, and HPPh$_2$ in methylene chloride at ambient temperature for 3 h yields the phosphine ligand-substituted complex. The IR and ^{13}C NMR spectra indicate that the phosphine-substituted compound has an analogous structure to that of VI.

L = PMe$_3$, PPh$_3$. HPPh$_2$
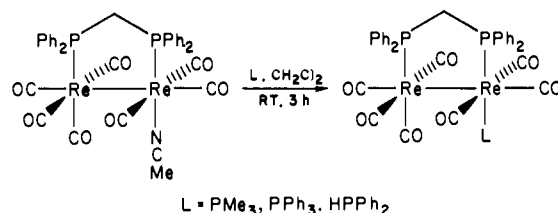
Reaction of VI with Phenylacetylene. Refulx of VI$_a$ in methylene chloride in the presence of phenylacetylene for 3 h leads to formation of two isomers (65:35) of (μ-H)Re$_2$(CO)$_7$(μ-dppm)(η^1-C≡CPh). The major product is I$_b$. The minor product shows the same molecular ion peaks as those of I$_b$ in the field desorption mass spectrum. The ^{1}H NMR spectrum in CDCl$_3$ displays a doublet of doublets at δ −14.99 (J_{PH} = 12.1 and 8.4 Hz) and a triplet at δ 4.05 (J_{PH} = 10.0 Hz). The chemical shift and splitting pattern of the former are similar to those of the bridging hydride in I$_b$, and the latter may be assigned to the methylene protons of dppm. The ^{13}C NMR spectrum displays the six carbonyl peaks with a small coupling constant (0–6.8 Hz) and a carbonyl peak with a large coupling constant (J = 48.3 Hz), indicating that only one carbonyl is located trans to phosphorus. On the basis of these spectroscopic data, we propose that this isomer has the following structure

I$_b$'
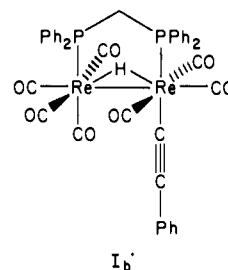
Reflux of I$_b$ in methylene chloride does not give I$_b$', and the reverse reaction does not occur either. Reflux of either I$_b$ or I$_b$' in toluene for 3 h yields II$_b$. Treatment of Re$_2$(CO)$_8$(μ-dppm) with 3 equiv of trimethylamine N-oxide in the presence of phenylacetylene at 50 °C also yields II$_b$.

Reflux of VI$_b$ in methylene chloride in the presence of phenylacetylene for 3 h only yields I$_d$.

Discussion

X-ray Crystal Structures of I$_d$ and III$_c$. The molecular structure of I$_d$ shown in Figure 2 reveals a distorted octahedral geometry about each rhenium atom. The mutual orientation of the rhenium coordination spheres about the Re–Re bond is intermediate between the staggered conformation as found in Re$_2$(CO)$_{10}$[16] and the eclipsed conformation observed in (μ-H)Re$_2$(CO)$_6$(μ-dppm)(μ-OH)[3] and (μ-H)Re$_2$(CO)$_8$(μ-NC$_5$H$_4$).[17] A slight twist about the Re–Re bond relieves strain in the C(12)–phenyl interaction. A noneclipsed conformation also increases the distance between methyl groups (C(8) and C(11)) which are on the side of the plane defined by the two rhenium and two phosphorus atoms opposite the methylene bridgehead; these methyl groups would be brought into close contact by a fully eclipsed conformation. The upfield chemical shift of the bridging hydride by 3–5 ppm, as compared with that of II or (μ-H)Re$_2$(CO)$_6$(μ-dppm)(μ-OH),[3]

(16) Dahl, L. F.; Ishishi, E.; Rundle, R. E. *J. Chem. Phys.* **1957**, *26*, 1750.
(17) Nubel, P. O.; Wilson, S. R.; Brown, T. L. *Organometallics* **1983**, *2*, 515.

Scheme I
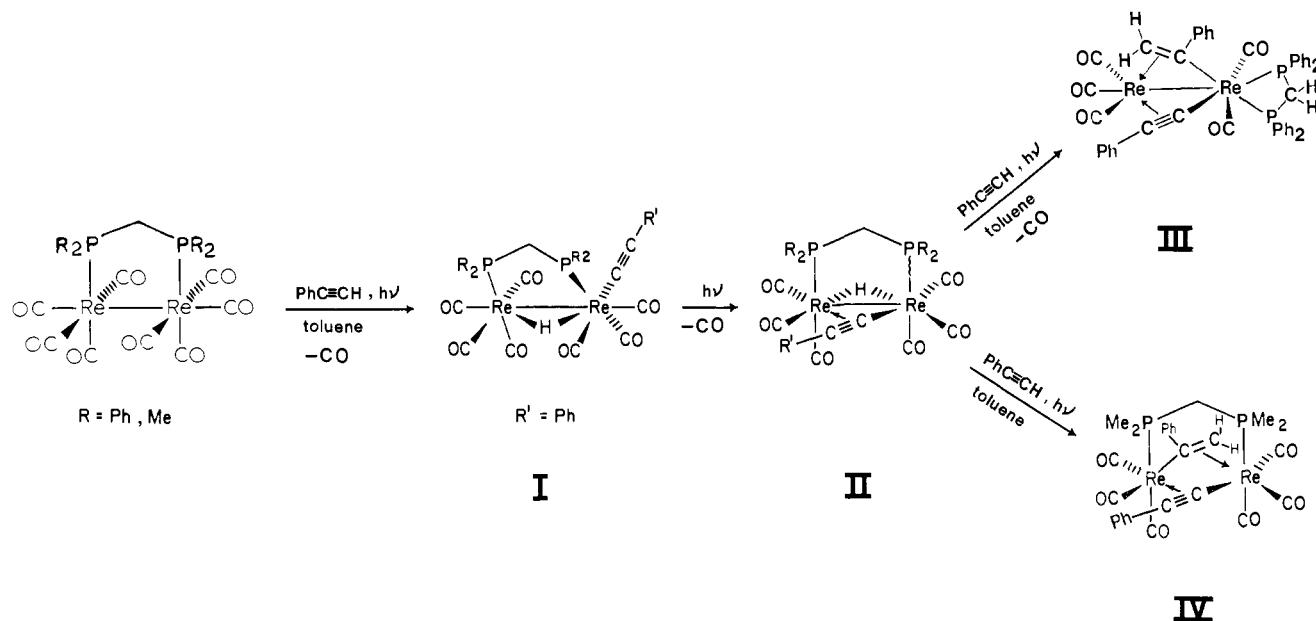
is possibly due to the long Re–Re distance.

The average of the Re–CO distances for carbonyl groups trans to another CO (1.978 Å) compares to that observed for the equatorial carbonyls of Re$_2$(CO)$_{10}$[18] and is significantly longer than the average for carbonyl groups that lack a trans CO (1.934 Å). The difference is probably due to competition for dπ-electron density between mutually trans carbonyls.

The phenylacetylido ligand is σ-bonded to Re(2), as evidenced by the Re(1)–Re(2)–C(13) bond angle (88.2 (2)°) and the linearity of the Re(2)–C(13)–C(14)–C(15) segment. The Re(2)–C(13) distance of 2.126 (7) Å is significantly longer than any of the Re–CO distances, indicating relatively little metal-to-ligand back-bonding. The C(13)–C(14) triple-bond distance (1.200 (9) Å) of σ-bonded phenylacetylide is close to that of free alkyne (1.204 (2) Å).[9a] The stretching vibration for phenylacetylide in the IR spectrum is observed at 2098 cm^{-1}.

The molecular structure of III$_c$ is shown in Figure 3. If each rhenium consists of 18 electrons, there should be a metal–metal single bond. The Re(1)–Re(2) bond distance of 2.895 (1) Å is much shorter than that for the Re–Re single bonds in (μ-H)-Re$_2$(CO)$_6$(μ-dppm)(μ-OH) (3.030 (1) Å),[3] Re$_2$(CO)$_8$(μ-η^1,η^3-CHCHCMe$_2$) (3.058 (1) Å),[19] and (μ-H)Re$_2$(CO)$_6$(μ-dppm)(μ-NC(H)Me) (3.035 (3) Å),[20] but it is close to the Re–Re double-bond distance in (μ-H)$_2$Re$_2$(CO)$_8$ (2.896 (3) Å)[21] and (μ-H)$_2$Re$_2$(CO)$_6$(μ-dppm) (2.893 (2) Å).[20] The shortened bond length is probably due to the bridging alkynyl-alkenyl ligands. The μ-η^1,η^2-phenylacetylido ligand (Re(1)–C(6)–C(7)–C(8)) has the trans bent configuration as observed in most of the bridging acetylido ligands.[9c,22] The phenylacetylido ligand shows an elongated carbon-carbon triple bond (1.24 (2) Å) compared to the σ-phenylacetylide of I$_a$ (1.200 (9) Å), presumably as a result of π-coordination to Re(2). The long bond length between Re(2) and C(7) (2.48 (2) Å) is consistent with the corresponding bond distance in Pt$_2$(μ-η^1,η^2-C≡CPh)(μ-SiMe$_2$)(η^1-C≡CPh)(PR$_3$)$_2$ (2.47(1) Å).[22] The C(2)–Re(1)–P angles are 158.9 (5)° and 90.1 (5)°, respectively, indicating that the doublet of doublets in the ^{13}C NMR spectrum of III$_c$ corresponds to the C(2) carbon.

Photochemical Reaction Mechanisms. The photochemical reaction of Re$_2$(CO)$_{10}$ with alkyne very likely proceeds via homolytic metal–metal bond cleavage, as in reactions with PR$_3$, pyridine, and alkenes.[23] Photolysis of Re$_2$(CO)$_8$(μ-dppm) undoubtedly also results in homolytic metal–metal bond cleavage as a major photoprocess. The diradical species formed in this process abstracts chlorine from carbon tetrachloride to yield Cl-(OC)$_4$RePPh$_2$CH$_2$Ph$_2$PRe(CO)$_4$Cl (see Experimental Section).[24] We know that chlorine atom transfer from CCl$_4$ to ·Re(CO)$_5$ occurs with a large rate constant (3.9 × 10^7 M^{-1} s^{-1}).[25] Thus chlorine atom transfer can compete with the expected rapid recombination to re-form the Re–Re bond. The photochemical reaction of Re$_2$(CO)$_8$[μ-(L-L)] with alkyne proceeds at less than one-sixth the rate of that with carbon tetrachloride. The dominant product in the early stage of the photochemical reaction, which is the result of loss of one carbonyl, is the same as that from the thermal reaction of the alkyne with Re$_2$(CO)$_7$(μ-dppm)(NCMe), indicating that loss of CO is the major reaction pathway. Presumably reaction of the transient diradical with alkyne is sufficiently slow that it does not compete with recombination. The alkyne reaction thus follows the slower CO dissociation path. The order of appearances of products as the reaction of Re$_2$(CO)$_8$-(μ-dppm) with phenylacetylene proceeds suggests that the reactions are consecutive: Re$_2$(CO)$_8$(μ-dppm) → I$_b$ → II$_b$ → III$_b$ (Scheme I). The observed pseudo-first-order behavior in reactions of the successive intermediates with phenylacetylene is consistent with this simple scheme.

The fact that I$_b$ is formed first in the reaction, to subsequently go on to II$_b$, indicates that II$_b$ is not formed as a primary photoproduct. A primary photoproduct that involves loss of one CO from *each* Re is probably not formed in the reaction, because this would be expected to lead directly to II$_b$. The analogous compound, (μ-H)Re$_2$(CO)$_8$(μ-C≡CPh), is formed upon thermal reaction of (μ-H)Re$_2$(CO)$_8$(μ-CH=CHR) with phenylacetylene,[15] or photochemical reactions of Re$_2$(CO)$_{10}$ with phenylacetylene.

The formation of I$_b$ from VI$_a$ and phenylacetylene in a thermal reaction suggests that alkyne substitution for CO may occur before the C–H oxidative addition. The η^2 interaction of the σ-alkynyl

(18) Churchill, M. R.; Amoh, K. N.; Wasserman, H. J. *Inorg. Chem.* **1981**, *20*, 1609.

(19) Green, M.; Orpen, A. G.; Schaverien, C. J.; Williams, I. D. *J. Chem. Soc., Chem. Commun.* **1983**, 1399.

(20) (a) Mays, M. J.; Prest, D. W.; Raithby, P. R. *J. Chem. Soc., Chem. Commun.* **1980**, 171. (b) *J. Chem. Soc., Dalton Trans.* **1982**, 2021.

(21) Bennett, M. J.; Graham, W. A. G.; Hoyano, J. K.; Hutcheon, W. L. *J. Am. Chem. Soc.* **1972**, *94*, 6232.

(22) Ciriano, M.; Howard, J. A. K.; Spencer, J. L.; Stone, F. G. A.; Wadepohl, H. *J. Chem. Soc., Dalton Trans.* **1979**, 1749.

(23) Nubel, P. O.; Brown, T. L. *J. Am. Chem. Soc.* **1984**, *106*, 644 and references therein.

(24) In the photochemical reaction of Re$_2$(CO)$_8$(μ-dppm) in carbon tetrachloride, there are two more minor products: one is Re$_2$(CO)$_6$(μ-dppm)-(μ-Cl)$_2$ and the other is unidentified. Further related reactions are under investigation.

(25) Meckstroth, W. K.; Walters, R. T.; Waltz, W. L.; Wojcicki, A.; Dorfman, L. M. *J. Am. Chem. Soc.* **1982**, *104*, 1842.

Scheme II

IV$_d$: R' = Ph   **VIII**
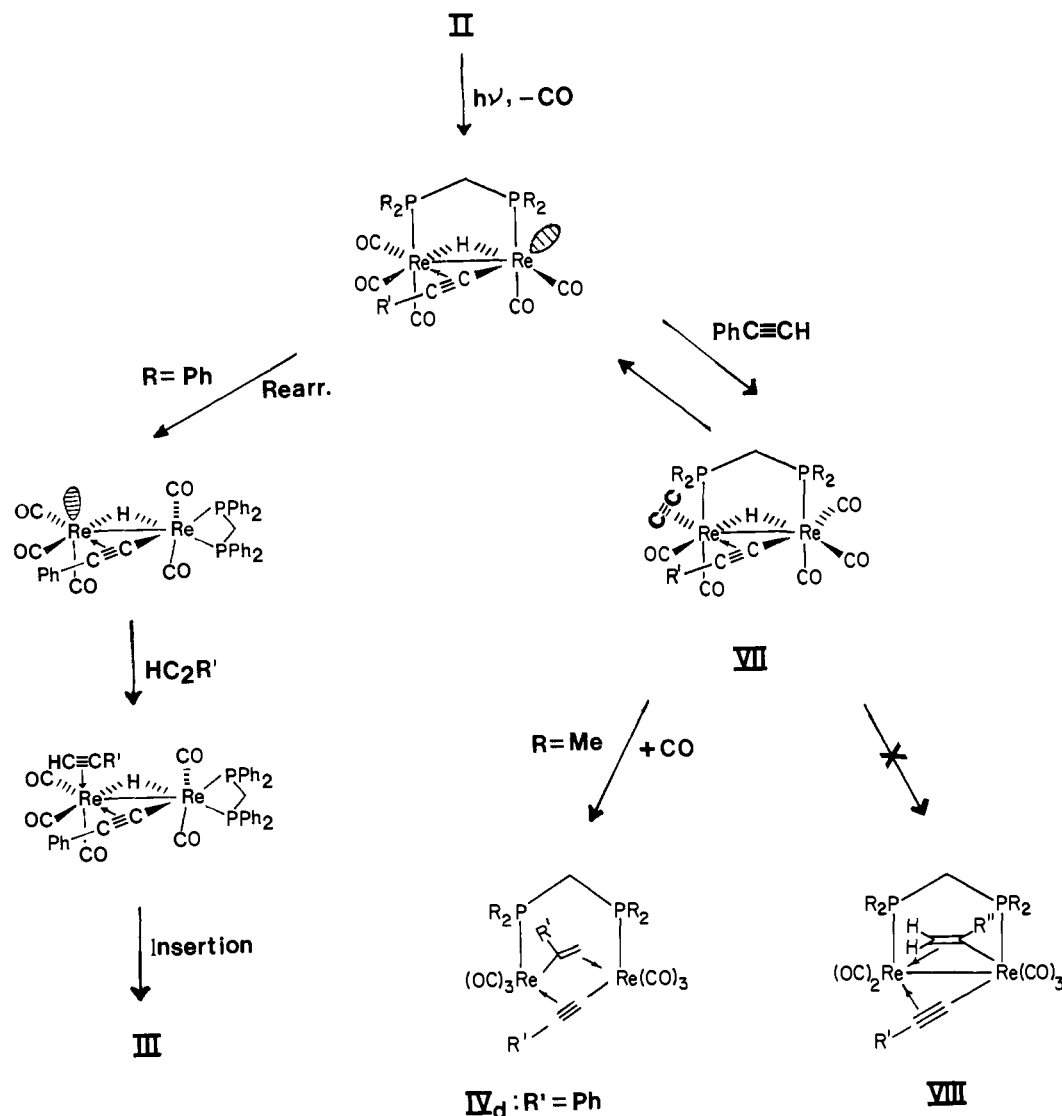
ligand upon loss of CO on the second metal center gives II$_b$. Formation of IV will be discussed later.

Rearrangement of dppm Coordination. Formation of V in the reaction of II$_b$ with PPh$_3$ is believed to occur via simple PPh$_3$ substitution for CO. The analogous, comparatively more rapid process has been observed for (μ-H)Re$_2$(CO)$_8$(μ-C≡CPh).[15] Location of PPh$_3$ trans to the phosphorus atom of dppm is expected in terms of steric preference, as observed in the formation of Re$_2$(CO)$_7$(dppm)(PMe$_3$) and Re$_2$(CO)$_6$(μ-dppm)$_2$,[26] wherein the phosphorus atoms are in trans positions. In the reaction of II$_b$ with phenylacetylene or acetylene, coordination of dppm undergoes rearrangement to form a chelate in III$_b$ or III$_c$. It is not clear how or why this unusual rearrangement occurs. A possible pathway is shown in Scheme II; it is proposed that the alkyne-substituted intermediate, VII, does not undergo alkynyl insertion into the Re–H bond to form a compound such as VIII because of steric hindrance. Continuous UV irradiation could eventually result in photodissociation of the phosphine, leading to rearrangement to give a chelating ligand. During this rearrangement, the Re–Re bond may be maintained by the bridging alkynyl ligand. In a successive step, one alkyne may occupy the empty site and undergo insertion into the Re–H bond to yield III$_b$ or III$_c$. It is noteworthy that the internal alkenyl isomer, Re$_2$-(CO)$_5$(dppm)(μ-η^1,η^2-CH=CHPh)(μ-η^1,η^2-C≡CPh), has not been observed. In the reaction of (μ-H)Re$_2$(CO)$_8$(μ-py) with

phenylacetylene, the terminal alkenyl complex, Re$_2$(CO)$_7$(μ-py)(μ-C(Ph)=CH$_2$), is also a major product.[27]

In contrast, coordination of dmpm does not undergo rearrangement in the reaction of II$_d$ with phenylacetylene. Instead, IV has been produced probably via phenylacetylene insertion into the Re–H bond, CO substitution, and metal–metal bond cleavage. Photodissociation of the phosphine of dmpm does not occur, possibly because of a high rhenium–phosphine bond energy resulting from electron donation from the methyl groups on phosphine. The yields of IV$_{a,b}$ are negligible when the bridging ligand is dppm because the rearrangement reaction to yield III is quite rapid.

Fluxional Behavior of the Bridging Alkynyl Ligand. It has been established that the alkenyl ligand of (μ-H)Os$_3$(CO)$_{10}$(μ-C(R)-=CHR')[28] or (μ-H)Re$_2$(CO)$_8$(μ-CH=CHR)[23] undergoes a rapid fluxional process at room temperature in which the σ and π bonds of the μ-alkenyl group are rapidly interchanged between two bridged metal atoms. Similar behaviors of the bridging alkynyl ligand in (μ-H)Re$_2$(CO)$_8$(μ-C≡CPh)[15] and (μ-H)$_2$Os$_3$(μ_3-alkyne)(CO)$_9$[29] have been reported. However, the variable temperature ^{13}C NMR spectra that provide direct evidence for ligand

(26) Lee, K.-W.; Brown, T. L. *Organometallics*, in press.

(27) Nubel, P. O. Ph.D. Thesis, University of Illinois at Urbana-Champaign, 1983.

(28) (a) Shapley, J. R.; Richter, S. I.; Tachikawa, M.; Keister, J. B. *J. Organomet. Chem.* **1975**, *94*, C43. (b) Clauss, A. D.; Tachikawa, M.; Shapley, J. R.; Pierpont, C. G. *Inorg. Chem.* **1981**, *20*, 1528.

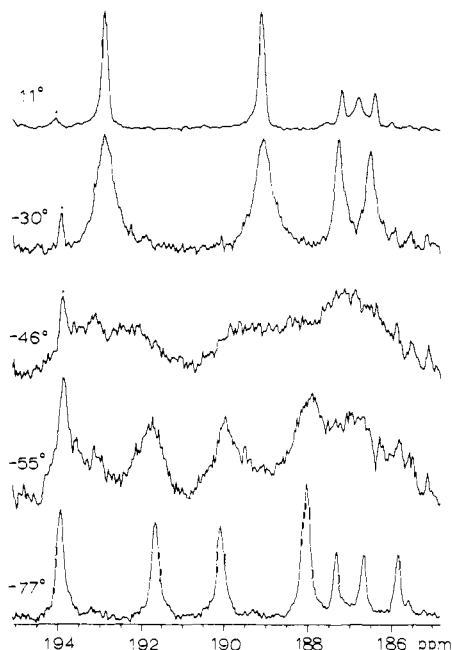(29) Deeming, A. J. *J. Organomet. Chem.* **1978**, *150*, 123.

Figure 6. Variable-temperature ^{13}C NMR spectra of $(\mu\text{-H})Re_2(CO)_6$-$(\mu\text{-dppm})(\mu\text{-}\eta^1,\eta^2\text{-C}\equiv\text{CH})$ (II$_a$) in the carbonyl region. The peak marked with an asterisk is due to an impurity.

fluxionality have not been obtained. We have obtained the variable temperature ^{13}C NMR spectra of II$_a$.

As shown in Figure 6, only three carbonyl peaks of equal intensity are observed above 11 °C. As the temperature is lowered, the peaks coalesce at −46 °C and finally split into six carbonyl peaks (δ 193.9 (s), 191.7 (s), 190.1 (s), 188.0 (s), 187.7 (d, J_{PC} = 63.9 Hz), 186.2 (d, J_{PC} = 75.6 Hz)). These results indicate that the alkynyl ligand of II$_a$ undergoes a fluxional process.
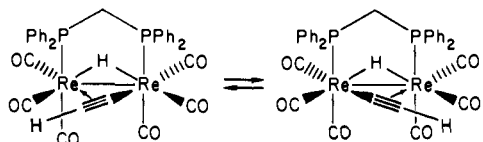
The $\Delta G^{\ddagger}_c$ value estimated from the coalescence temperature is 10.5 kcal/mol, quite similar to the values observed for alkenyl ligands (10.0–12.7 kcal/mol).[23,28]

In summary, we have reported here the photochemical reactions of $Re_2(CO)_8[\mu\text{-(L-L)}]$ with alkynes which yield I, II, III, and IV. Dissociation of CO has been proposed as the dominant initial pathway for reaction. The reactions are consecutive: Re_2-$(CO)_8(\mu\text{-dppm}) \rightarrow I \rightarrow II \rightarrow III$. We have also reported the thermal reactions of $Re_2(CO)_7[\mu\text{-(L-L)}](NCMe)$ with phenyl-acetylene, which quantitatively yields I or II depending on reaction conditions. I provides the first example of μ-hydrido, η^1-alkynyl polynuclear compounds (G bonding mode in Figure 1). The molecular structure of I$_d$ shows the presence of η^1-alkynyl ligand. The molecular structure of III$_c$ exhibits bridging alkenyl–alkynyl groups in a dinuclear complex with an unusual dppm chelate. The bridging alkynyl ligand of II undergoes a rapid fluxional process.

Experimental Section

General. All reactions were carried out under an argon atmosphere. Photochemical reactions were performed by irradiation with a General Electric 275-W sunlamp with Pyrex Schlenk vessels, or with an Oriel 17 mA mercury–argon lamp, with a Quartz vessel. Benzene and toluene were distilled from CaH₂ under nitrogen and degassed prior to use. Acetonitrile was distilled under nitrogen from P₂O₅ immediately prior to use. Dirheniumdecacarbonyl, bis(diphenylphosphino)methane(dppm) (Pressure Chemical Co.), bis(dimethylphosphino)methane(dmpm) (Strem Chemicals), and triphenylphosphine (Aldrich) were all used without further purification. Phenylacetylene (Aldrich), Acetylene (Union Carbide), and ¹³CO (Monsanto) were used without further purification. Anhydrous trimethylamine *N*-oxide, Me₃NO, was prepared by vacuum sublimation of the dihydrate, Me₃NO·2H₂O (Aldrich, 98%).

Reagent grade solvents (hexane, toluene, CH₂Cl₂, ethyl acetate) were also used without purification for chromatography and recrystallization. Silica gel (70–230 mesh, EM Reagents) was employed for column chromatography. Preparative TLC plates (20 × 20 cm, 2.0 mm silica with UV₂₅₄ fluorescent indicator) were obtained from Brinkmann Instruments, Inc.

Infrared spectra were obtained on a Beckmann IR-4240 spectrophotometer. Fast atom bombardment (FAB) and field desorption mass spectra (FDMS) were obtained with Finnigan-MAT 731 and ZAB-HF mass spectrometers in the Mass Spectrometry Laboratory, School of Chemical Sciences, University of Illinois. ¹H NMR and ¹³C NMR were obtained with use of a Nicolet NIC-360 instrument at 360 and 90 MHz, respectively. The carbonyl region of ¹³C NMR spectra was obtained with use of ¹³CO-enriched compounds. The enrichment was carried out on the starting materials [Re₂(CO)₈(μ-dppm) and -(μ-dmpm)] by photolysis under ¹³CO-enriched (99%) atmosphere for 12 h. Spectra were recorded at ambient temperature except where indicated. Data are referred to tetramethylsilane at δ 0. Elemental analyses were performed by the University of Illinois Microanalytical Laboratory.

Re₂(CO)₈(μ-dppm) and -(μ-dmpm) were prepared from Re₂(CO)₁₀ as previously described.[3]

Photochemical Reactions of Re₂(CO)₁₀ with Acetylene and Phenyl-acetylene. Re₂(CO)₁₀ (0.150 g, 0.230 mmol) was added into a 50-mL Schlenk flask containing toluene (20 mL) and phenylacetylene (0.235 g, 2.300 mmol). After being degassed, the solution was irradiated at ambient temperature for 3 h. The major product, $(\mu\text{-H})Re_2(CO)_8(\mu\text{-C}\equiv\text{CPh})$,[15] was isolated by silica gel packed column chromatography and characterized by IR, ¹H NMR, and FDMS. Because of decomposition on silica gel supports, the yield could not be determined. The minor product(s) could not be isolated because of rapid decomposition on TLC supports.

The corresponding reaction with acetylene was performed by a similar procedure as described above, yielding $(\mu\text{-H})Re_2(CO)_8(\mu\text{-C}\equiv\text{CH})$.

Photochemical Reactions of Re₂(CO)₈(μ-dppm) and -(μ-dmpm) with Acetylene and Phenylacetylene. Re₂(CO)₈(μ-dppm) (0.098 g, 0.100 mmol), an excess of phenylacetylene, and toluene (10 mL) were added into a 50-mL Schlenk flask. The solution was degassed and irradiated at ambient temperature for 12 h. After the liquid portion was removed under reduced pressure, the pure products were separated as yellow solids on silica gel coated preparative TLC plates with methylene chloride and hexane (3:1) and recrystallized from the solvent system. I$_b$ (0.018 g, 17%), II$_b$ (0.047 g, 46%), and III$_b$ (0.027 g, 25%) were isolated. Anal. Calcd for C₄₀H₂₈O₇P₂Re₂ (I$_b$): C, 45.54; H, 2.67. Found: C, 45.70; H, 2.71. Calcd for C₃₉H₂₈O₆P₂Re₂ (II$_b$): C, 45.61; H, 2.75. Found: C, 45.05; H, 2.76. Calcd for C₄₆H₃₄O₅P₂Re₂ (III$_b$): C, 50.18; H, 3.11. Found: C, 50.02; H, 3.14.

The corresponding reaction of Re₂(CO)₈(μ-dmpm) (0.074 g, 0.101 mmol) was also carried out as in the previous procedure. I$_d$ (0.019 g, 23%), II$_d$ (0.032 g, 41%), and IV$_d$ (0.017 g, 19%) were isolated. The IR and ¹³C NMR spectra of I$_d$ and II$_d$ are similar to those of I$_b$ and II$_b$. Anal. Calcd for C₂₇H₂₆O₆P₂Re₂ (IV$_d$): C, 36.81; H, 2.97. Found: C, 36.92; H, 2.99. IR (ν_{CO}, toluene) 2030 (s), 1996 (m), 1951 (s), 1932 (m), 1907 (m), 1880 cm⁻¹ (s). ¹H NMR (CDCl₃) δ 7.81 (d, 2 H, *J* = 7.6 Hz), 7.38 (t, 2 H, *J* = 7.4 Hz), 7.07–7.28 (m, 7 H), 4.67 (s, 1 H), 1.68–1.97 (m, 8 H), 1.15 (t, 6 H, *J* = 7.2 Hz). ¹³C NMR (CDCl₃) δ 196.2 (d, 1 C, J_{PC} = 8.2 Hz) 195.7 (d, 1 C, J_{PC} = 6.9 Hz), 195.5 (d, 1 C, J_{PC} = 7.8 Hz), 192.9 (s, 1 C), 189.1 (d, 1 C, J_{PC} = 72.5 Hz), 187.6 (d, 1 C, J_{PC} = 65.7 Hz). FABMS *m/e* 882. The spectroscopic data for I, II, and III are listed in Tables I, II and III, respectively. The yield depends on the reaction time.

Preparation of Re₂(CO)₇(NCMe)(μ-dppm) and -(μ-dmpm). In a typical reaction, Re₂(CO)₈(μ-dppm) (0.098 g, 0.100 mmol) and distilled acetonitrile (20 mL) were added into a 50-mL Schlenk flask equipped with a dropping funnel containing anhydrous trimethylamine *N*-oxide (0.010 g, 0.133 mmol) dissolved in acetonitrile (5 mL). The trimethylamine *N*-oxide solution was dropped into Re₂(CO)₈(μ-dppm) solution, and the mixture was stirred at ambient temperature for 24 h. The solvent was removed under reduced pressure. The pure yellow product, Re₂(CO)₇(μ-dppm)(NCMe) (90%), was isolated by recrystallization from methylene chloride and hexane. Anal. Calcd for C₃₄H₂₅NO₇P₂Re₂: C, 41.09; H, 2.54; N, 1.41. Found: C, 41.10; H, 2.61; N, 1.21. IR (ν_{CO}, toluene) 2042 (m), 1992 (m), 1953 (s), 1935 (s, sh), 1920 (m), 1900 (m), 1884 cm⁻¹ (s). ¹H NMR (CDCl₃) δ 7.29–7.42 (m, 20 H), 4.15 (t, 2 H, J_{PH} = 9.9 Hz), 2.38 (s, 3 H). ¹³C NMR (CDCl₃) δ 209.0 (d, 2 C, J_{PC} = 6.4 Hz), 206.9 (d, 2 C, J_{PC} = 8.6 Hz), 199.4 (d, 1 C, J_{PC} = 48.9 Hz), 193.5 (d, 1 C, J_{PC} = 7.0 Hz), 192.6 (d, 1 C, J_{PC} = 3.6 Hz). FABMS *m/e* 995.

The corresponding reaction of Re₂(CO)₈(μ-dmpm) yields Re₂(CO)₇-(μ-dmpm)(NCMe) characterized by IR and ¹H NMR. However, the pure product could not be isolated due to decomposition. IR (ν_{CO}, tol-

640 *J. Am. Chem. Soc., Vol. 107, No. 3, 1985*

Lee et al.

uene) 2032 (s), 1977 (s), 1940 (s, sh), 1928 (s), 1922 (s, sh), 1892 (s), 1870 cm^{-1} (s). ^{1}H NMR (CDCl$_3$) δ 2.88 (s).

Reaction of Re$_2$(CO)$_7$(μ-dppm)(NCMe) with PMe$_3$, PPh$_3$, and HPPh$_2$. In a typical reaction, Re$_2$(CO)$_7$(μ-dppm)(NCMe) (0.110 g, 0.110 mmol), an excess amount of triphenylphosphine, and methylene chloride (20 mL) were added into a 50-mL flask and the mixture was stirred at ambient temperature for 3 h. The pure yellow solid product was isolated by preparative TLC and recrystallization with hexane and methylene chloride. Re$_2$(CO)$_7$(μ-dppm)(PPh$_3$): IR (ν_{CO}, toluene) 2053 (m), 1975 (s, sh), 1963 (vs), 1936 (m, sh), 1917 (s), 1900 (m), 1883 cm^{-1} (s); ^{1}H NMR (CDCl$_3$) δ 4.43 (t, 2 H, J_{PH} = 9.7 Hz); FDMS m/e 1216. Re$_2$(CO)$_7$(μ-dppm)(HPPh$_2$): IR (ν_{CO}, toluene) 2045 (m), 1993 (m), 1985 (m, sh), 1956 (vs), 1942 (m, sh), 1923 (m), 1904 (m), 1882 cm^{-1} (s); ^{1}H NMR (CDCl$_3$) δ 7.02 (dd, 1 H, J_{PH} = 357.7 and 8.5 Hz), 4.37 (t, 2 H, J_{PH} = 9.8 Hz); ^{13}C NMR (CDCl$_3$) δ 205.1 (t, 2 C, J_{PC} = 8.5 Hz) 204.8 (d, 2 C, J_{PC} = 8.2 Hz), 197.9 (d, 1 C, J_{PC} = 49.1 Hz), 195.9 (t, 1 C, J_{PC} = 7.1 Hz), 191.3 (d, 1 C, J_{PC} = 6.4 Hz); FDMS m/e 1140. Re$_2$(CO)$_7$(μ-dppm)(PMe$_3$): IR (ν_{CO}, toluene) 2043 (m), 1980 (m, sh), 1973 (m), 1955 (vs), 1936 (m, sh), 1918 (m), 1895 (s), 1877 cm^{-1} (s); ^{1}H NMR (CDCl$_3$) δ 7.18–7.60 (m, 20 H), 4.91 (t, 2 H, J_{PH} = 5.2 Hz); FDMS m/e 1030.

Reaction of Re$_2$(CO)$_7$(μ-dppm)(NCMe) and Re$_2$(CO)$_7$(μ-dmpm)-(NCMe) with Phenylacetylene. In a typical reaction, Re$_2$(CO)$_7$(μ-dppm)(NCMe) (0.055 g, 0.055 mmol), an excess amount of phenylacetylene (0.3 mL), and methylene chloride (20 mL) were added into a 50-mL flask equipped with a refluxing condenser. The mixture was refluxed for 3 h. I$_b$ and I$_b$′ were isolated in 55 and 30% yield, respectively, by silica gel coated preparative TLC with hexane and methylene chloride. I$_b$′: IR (ν_{CO} and $\nu_{C≡C}$, toluene) 2106 (m), 2098 (w, sh), 2030 (s), 2000 (s, sh), 1993 (vs), 1972 (s), 1943 (s), 1926 cm^{-1} (s); ^{1}H NMR (CDCl$_3$) δ 7.00–7.45 (m, 25 H), 4.05 (t, 2 H, J_{PH} = 10.0 Hz), −14.99 (dd, 1 H, J_{PH} = 12.1 and 8.4 Hz); ^{13}C NMR (CDCl$_3$) δ 193.3 (s, 1 C), 191.1 (d, 2 C, J_{PC} = 3.5 Hz), 185.0 (d, 2 C, J_{PC} = 6.8 Hz), 183.2 (s, 1 C), 181.6 (d, 1 C, J_{PC} = 48.3 Hz); FDMS m/e 1056.

The equivalent reaction of Re$_2$(CO)$_7$(μ-dmpm)(NCMe) was carried out. I$_d$ was isolated in 80% yield. Any other isomer of I$_d$ was not found.

Thermal and Photochemical Reactions of I$_b$ and II$_b$. I$_b$ (0.063 g, 0.060 mmol) and toluene (20 mL) were added into a 50-mL flask equipped with a refluxing condenser. The mixture was refluxed for 3 h. II$_b$ was isolated in 85% yield by preparative TLC with hexane and methylene chloride (25:75). UV irradiation of I$_b$ in toluene at ambient temperature also yielded II$_b$ (0.046 g, 75%).

II$_b$ (0.072 g, 0.070 mmol) was added to a 50-mL Schlenk flask containing toluene (15 mL) and phenylacetylene (0.5 mL). After being degassed, the solution was irradiated by a sunlamp for 12 h. All liquid was removed under reduced pressure. The pure product (III$_b$) was isolated in 50% yield by preparative TLC with methylene chloride and hexane (3:1) and recrystallized from the same solvent system. The equivalent irradiation of II$_b$ in the presence of acetylene was carried out for 18 h. The pure product (III$_c$) was obtained by the same procedure described above. Calcd for C$_{40}$H$_{30}$O$_5$Re$_2$P$_2$ (III$_c$): C, 46.87; H, 2.95. Found: C, 46.31; H, 2.85.

II$_b$ (0.051 g, 0.050 mmol), triphenylphosphine (0.052 g, 0.200 mmol), and toluene (20 mL) were added to a 50-mL flask equipped with a refluxing condenser. The mixture was refluxed for 3 h. The product, (μ-H)Re$_2$(CO)$_5$(μ-dppm)(μ-C≡CPh)(PPh$_3$), was isolated in 70% yield on preparative TLC. Anal. Calcd for (μ-H)Re$_2$(CO)$_5$(μ-dppm)(μ-C≡CPh)(PPh$_3$): C, 53.33; H, 3.44; P, 7.37. Found: C, 53.51; H, 3.66; P, 7.55. IR (ν_{CO}, toluene) 2026 (s), 1950 (m, sh), 1927 (s, br), 1878 cm^{-1} (s); ^{1}H NMR (CDCl$_3$) δ 3.72 (q, 1 H, J_{PH} = 10.5 Hz), 2.87 (q, 1 H, J_{PH} = 10.5 Hz), −11.64 (q, 1 H, J_{PH} = 7.5 Hz); ^{13}C NMR (CDCl$_3$) δ 199.7 (s, 1 C), 194.5 (t, 1 C, J_{PC} = 8.0 Hz), 192.0 (d, 1 C, J_{PC} = 3.9 Hz), 190.5 (d, 1 C, J_{PC} = 9.0 Hz), 186.5 (d, 1 C, J_{PC} = 76.0 Hz); FDMS m/e 1262 based on ^{187}Re.

Photochemical Reaction of Re$_2$(CO)$_8$(μ-dppm) with Carbon Tetrachloride. Re$_2$(CO)$_8$(μ-dppm) (0.085 g, 0.087 mmol) and carbon tetrachloride (10 mL) were added into a 50-mL Schlenk flask. The solution was degassed and irradiated at ambient temperature for 3 h. The pure products were separated as white solids on silica gel coated preparative TLC plates with methylene chloride and hexane (3:1) and recrystallized from the same solvent system. Cl(OC)$_4$RePPh$_2$CH$_2$Ph$_2$PRe(CO)$_4$Cl (70%) and Re$_2$(CO)$_6$(μ-dppm)(μ-Cl)$_2$^{3} (10%) were isolated. There was an unidentified product ($\sim$10%) which decomposed on TLC plate. Anal. Calcd for a major product (C$_{33}$H$_{22}$Cl$_2$P$_2$O$_8$Re$_2$): C, 37.69; H, 2.11. Found: C, 37.37; H, 2.12. IR (toluene) ν_{CO} 2106 (w), 2016 (m, sh), 2005 (s), 1952 cm^{-1} (m); ^{1}H NMR (CD$_2$Cl$_2$) δ 7.24–7.58 (m, 20 H), 4.89 (t, 2 H, J_{PH} = 5.5 Hz); FDMS M$^+$ at m/e 1056 based on ^{187}Re and ^{37}Cl.

Kinetics Studies. The photochemical reactions were carried out in a 0.2-mm IR cell which was placed 10 cm from a 275 W GE sunlamp. Solutions were maintained at ambient temperature during photolysis by

forced-air cooling of the IR cell. The extinction coefficients for Re$_2$-(CO)$_8$(μ-dppm), I$_b$, II$_b$, and III$_b$ which were determined with authentic samples were 2910, 1175, 4730, and 1070 M^{-1} cm^{-1} at 2073, 2106, 2046, and 1887 cm^{-1}, respectively. The absorbances were measured in IR spectra taken at 5–10 min interval. The reaction of 1.53 × 10^{-2} M Re$_2$(CO)$_8$(μ-dppm) with 0.360 M phenylacetylene was carried out. The concentration vs. time measurement was shown in Figure 4. The rate of disappearance of Re$_2$(CO)$_8$(μ-dppm) was also measured with 1.31 × 10^{-2} M Re$_2$(CO)$_8$(μ-dppm) and 0.066 and 0.131 M phenylacetylene. The linear relationship between ln [M] and time for each reactant is shown in Figure 5.

X-ray Crystal Structure Determination of I$_d$ and III$_c$. Single crystals of I$_d$ and III$_c$ were each mounted with epoxy on a glass fiber for data collection at ambient temperature with graphite-monochromated Mo Kα radiation (λ 0.71073 Å) on an Enraf-Nonius CAD-4 diffractometer.

I$_d$: the crystal used for data collection was bound by four pairs of faces (100, 110, 1$\bar{1}$0, and 001) with approximate face-to-center distances of 0.10, 0.30, 0.30, and 0.33 mm, respectively. Unit cell parameters (determined from 25 reflections with 36° < 2θ < 40°) are a = 12.594 (1) Å, b = 11.075 (1) Å, c = 18.461 (3) Å, β = 105.88 (1)°, V = 2476.8 (9) Å,^{3} and D_{calcd} = 2.163 g cm^{-3}. There are four molecules in the unit cell which belongs to the monoclinic space group $P2_1/c$, No. 14 (systematic absences: 0k0, k ≠ 2n; h0l, l ≠ 2n). A total of 7215 reflections were measured at speeds of 3.4 to 5.0° min^{-1} with θ–2θ scans over a range of (1.00 + 0.35 tan θ)° for 2° < 2θ < 60°. The analytical absorption correction (μ = 100.6 cm^{-1}) varied from 0.04 to 1.00. The intensities of three standard reflections ($\bar{2}$10$\overline{14}$, 9 3$\overline{11}$, and 5 6$\overline{12}$) measured after every hour of X-ray exposure time fluctuated by a maximum of 4.6% thus indicating general crystal stability.

The atomic coordinates of the two rhenium atoms were determined by direct methods (MULTAN80), and the remaining non-hydrogen atoms were located by standard Fourier techniques. The methyl, methylene, and phenyl hydrogen atoms were located on a difference Fourier map and were included in the structure factor calculation at idealized positions (d_{C-H} = 0.95 Å) with isotropic B values of 1.2 times the B_{eq} value of the carbon atoms to which they are bonded. An attempt to locate the bridging hydride ligand by difference Fourier techniques was unsuccessful. In the final cycle of full-matrix least-squares refinement, which included 280 parameters and 5229 observed reflections ($I > 3\sigma(I)$) for a reflection/parameter ratio of 18.7/1, no parameter shifted by more than 0.02 σ's. The final residual values were R = 0.034 and R_w = 0.046, and the goodness-of-fit indicator was 1.28. The weighting scheme was based on counting statistics (p = 0.05) and showed no dependence of $\Delta F/\sigma$ on either the magnitude of F or the value of θ. The largest peak on the final difference map (0.89 e Å^{-3}) was 0.98 Å away from one of the ruthenium atoms.

III$_c$: The crystal used for data collection was bound by six pairs of faces (010, 001, 111, $\bar{1}$11, 1$\bar{1}$1, and 11$\bar{1}$) with face-to-center distances of 0.16, 0.10, 0.17, 0.17, 0.17, and 0.17 mm, respectively. Unit cell parameters (determined from 25 reflections with 28° < 2θ < 32°) are a = 12.743 (2) Å, b = 15.974 (2) Å, c = 35.174 (4) Å, V = 7160 (2) Å^3, and D_{calcd} = 1.902 g cm^{-3}. There are eight molecules in the unit cell which belongs to the orthorhombic space group, $Pbca$, No. 61 (systematic absences: 0kl, k ≠ 2n; h0l, l ≠ 2n; hk0, h ≠ 2n). A total of 6609 reflections were measured (2° < 2θ < 50°) with θ–2θ scans over a range of (1.00 + 0.35 tan θ)° at speeds ranging from 2.0 to 20.1° min^{-1}. The analytical absorption correction (μ = 72.8 cm^{-1}) varied from 0.62 to 1.00. The intensities of three standard reflections (0$\bar{6}$23, 4$\bar{7}$15, $\bar{9}$02) fluctuated by a maximum of 4.2% and thus indicated general crystal stability.

The positions of the rhenium atoms were determined by analysis of a Patterson map, and the remaining non-hydrogen atoms were located by standard Fourier techniques. Hydrogen atoms were included in the structure factor calculation at idealized positions (d_{C-H} = 0.95 Å) with isotropic B values of 1.2 times the B_{eq} value of the carbon atoms to which they are bonded. The final full-matrix least-squares refinement included positional and anisotropic thermal parameters for all non-hydrogen atoms. The refinement included 442 parameters and 3825 observed reflections ($I > 3\sigma(I)$) for a reflection/parameter ratio of 8.7/1 and produced residuals R = 0.055, R_w = 0.074, and GOF = 1.84. The weighting scheme was based on counting statistics (p = 0.05) and showed no dependence of $\Delta F/\sigma$ on either F or sin θ. The five largest peaks on the final difference map (1.7–2.3 e Å^{-3}) were all within 1.1 Å of a rhenium atom.

Atomic scattering factors and anomalous dispersion corrections for both compounds were taken from "International Tables for X-ray Crystallography".^{30} The selected intramolecular distances and angles

(30) "International Tables for X-ray Crystallography"; Kynoch Press: Birmingham, England, 1974; Vol. IV.

for I_d and III_c are given in Tables IV and V, respectively.

Registry No. Ia, 94090-56-9; Ib, 94090-57-0; Ib′, 94160-63-1; Ic, 94090-58-1; Id, 94090-59-2; IIa, 94090-60-5; IIb, 94111-25-8; IIc, 94136-21-7; IId, 94111-26-9; IIIa, 94136-23-9; IIIb, 94136-24-0; IIIc, 94136-25-1; IVa, 94111-27-0; IVb, 94111-28-1; IVc, 94136-22-8; IVd, 94111-29-2; V, 94111-30-5; VIa, 94136-27-3; VIb, 94136-26-2; Re$_2$-(CO)$_7$(μ-dppm)(PMe$_3$), 94111-31-6; Re$_2$(CO)$_7$(μ-dppm)(PPh$_3$), 94111-32-7; Re$_2$(CO)$_7$(μ-dppm)(HPPh$_2$), 94136-28-4; Cl-(OC)$_4$RePPh$_2$CH$_2$Ph$_2$PRe(CO)$_4$Cl, 94111-33-8; Re$_2$(CO)$_6$(μ-dppm)(μ-Cl)$_2$, 94111-34-9; Re$_2$(CO)$_8$(μ-dppm), 82292-83-9; Re$_2$(CO)$_8$(μ-dmpm), 88271-76-5; PPh$_3$, 603-35-0; PMe$_3$, 594-09-2; HPPh$_2$, 829-85-6; CCl$_4$, 56-23-5; acetylene, 74-86-2; phenylacetylene, 536-74-3.

Supplementary Material Available: Table A, atomic positional parameters for I_d; Table B, anisotropic thermal parameters for I_d; Table C, calculated hydrogen atom positions for I_d; Table D, atomic positional parameters for III_c; Table E, anisotropic thermal parameters for III_c; Table F, calculated hydrogen atom positions for III_c (12 pages). Ordering information is given on any current masthead page.

Supported Organoactinides. Surface Chemistry and Catalytic Properties of Alumina-Bound (Cyclopentadienyl)- and (Pentamethylcyclopentadienyl)thorium and -uranium Hydrocarbyls and Hydrides

Ming-Yuan He,[1a] **Guoxing Xiong,**[1b] **Paul J. Toscano, Robert L. Burwell, Jr.,*** and **Tobin J. Marks***

Contribution from the Department of Chemistry, Northwestern University, Evanston, Illinois 60201. Received July 10, 1984

Abstract: This contribution reports a detailed, quantitative investigation of surface chemistry and catalysis involving selected organoactinides and partially dehydroxylated (PDA) or dehydroxylated (DA) alumina supports. For the complexes Cp′$_2$M(CH$_3$)$_2$ and Cp′$_2$M(CD$_3$)$_2$ (Cp′ = η^5-(CH$_3$)$_5$C$_5$; M = Th, U), methane-evolving surface reaction pathways are identified as M–CH$_3$ protonolysis via surface OH (especially on PDA), Cp′ H atom abstraction, and intramolecular elimination of methane within M(CH$_3$)$_2$ units. This latter process is proposed on the basis of methylene transfer to acetone and some olefin metathesis activity to result in Al^{3+}-stabilized alkylidenes. Hydrogenolysis studies indicate that ca. 25% of the Cp′$_2$M(CH$_3$)$_2$/DA surface M–CH$_3$ groups are removable as methane; reduction of methyl chloride to methane confirms the presence of surface M–H groups produced by hydrogenolysis. The Cp′$_2$M(CH$_3$)$_2$/DA complexes are active catalysts for propylene hydrogenation following a variety of pretreatment conditions, with $N_t \approx 0.5$ s^{-1} in a flow reactor at −63 °C (about 10 times more active than typical Pt/SiO$_2$ catalysts under the same conditions). M = Th and U are comparable in hydrogenation activity, and CO poisoning experiments indicate that ca. 3% of the adsorbed molecules is catalytically active. Cp′$_2$M(CH$_3$)$_2$ complexes on PDA and silica gel are considerably less active catalysts. The Cp′$_2$M(CH$_3$)$_2$/DA systems are also active catalysts for ethylene polymerization and weakly active for butene isomerization. Experiments with Cp′$_2$Th[CH$_2$C(CH$_3$)$_3$]$_2$ and [Cp′$_2$Th(μ-H)H]$_2$ on DA reveal activity for propylene hydrogenation comparable to the Cp′$_2$M(CH$_3$)$_2$ systems. In contrast, more coordinatively saturated Cp$_3$UCH$_3$ and Cp$_3$Th(n-C$_4$H$_9$) (Cp = η^5-C$_5$H$_5$) are far less active, while Cp′Th(CH$_2$C$_6$H$_5$)$_3$ is far more active ($N_t \approx 10$ s^{-1}). Much of the stoichiometric and catalytic surface chemistry can be understood in terms of solution organoactinide reactivity patterns.

There is currently great interest in the structural, chemical, and catalytic properties of the unusual species formed when carbonyl and non-carbonyl transition-metal organometallic compounds are adsorbed on the surfaces of porous metal oxides such as γ-alumina, silica, magnesia, zeolites, etc.[2] In a number of cases, these supported species exhibit dramatic reactivity enhancements over the precursor molecules in homogeneous solution, and high catalytic activity for such processes as the hydrogenation, metathesis, isomerization, and polymerization of olefins is observed. Several of these organometallic/metal oxide systems are also of technological significance.[2,3] The accurate characterization of such highly reactive molecule/support complexes has presented a great challenge and, in all but a few cases, the present structural/mechanistic picture remains highly speculative.

In homogeneous solution, organoactinides display a rich variety of unusual stoichiometric and catalytic reactivity patterns.[4]

(1) (a) Visiting scholar on leave from the Research Institute of Petroleum Processing, Beijing, PRC. (b) Visiting scholar on leave from the Institute of Chemical Physics, Dalian PRC.

(2) (a) Yermakov, Yu. I. *J. Mol. Catal.* **1983**, *21*, 35–55 and references therein. (b) Basset, J. M.; Chaplin, A. *J. Mol. Catal.* **1983**, *21*, 95–108 and references therein. (c) Iwamoto, M.; Kusano, H.; Kagawa, S. *Inorg. Chem.* **1983**, *22*, 3365–3366 and references therein. (d) Yermakov, Yu. I.; Kuznetsov, B. N.; Zakharov, V. A. "Catalysis by Supported Complexes"; Elsevier: Amsterdam, 1981. (e) Bailey, D. C.; Langer, S. H. *Chem. Rev.* **1981**, *81*, 109–148. (f) Zakharov, V. A.; Yermakov, Yu. I. *Catal. Rev.—Sci. Eng.* **1979**, *19*, 67–103. (g) Hartley, F. R.; Vezry, P. N. *Adv. Organomet. Chem.* **1978**, *15*, 189–234. (h) Ballard, D. G. H. *J. Polym. Sci., Polym. Chem. Ed.* **1975**, *13*, 2191–2212. (i) Ballard, D. G. H. *Adv. Catal.* **1973**, *23*, 263–325.

(3) (a) Gavens, P. D.; Bottrill, M.; Kelland, J. W.; McMeeking, J. In "Comprehensive Organometallic Chemistry"; Wilkinson, G., Stone, F. G. A., Abel, E. W., Eds.; Pergamon Press: Oxford, 1982; Chapter 22.5. (b) Galli, P.; Luciani, L.; Cecchini, G. *Angew. Makromol. Chem.* **1981**, *94*, 63–89. (c) Karol, F. J.; Wu, C.; Reichle, W. T.; Maraschin, N. J. *J. Catal.* **1979**, *60*, 68–76. (d) Boor, J., Jr. "Ziegler-Natta Catalysts and Polymerizations"; Academic Press: New York, 1979; Chapters 6, 22. (e) Firment, L. E. *J. Catal.* **1983**, *82*, 196–212 and references therein.